轮胎动力学协同创新联盟
Tire Dynamics Collaborative Innovation Alliance

轮胎动力学通讯

2019年第4期 总第6期

Tire Dynamics Newsletters

外智大师班研讨会顺利召开

※ 相似法（复合滑移部分）

※ 浦林成山（山东）轮胎有限公司研发实力简介

※ 2019轮胎与车辆动力学院士论坛盛大召开

夯实行业创新发展的基础技术：轮胎动力学

目录

卷首语

夯实行业创新发展的基础技术——轮胎动力学 ……1

封面故事

2019轮学盟“外智大师班”研讨会顺利召开……3

技术前沿

1. Parameter Identification and Validation for Combined Slip Tire Models using a Vehicle Measurement System……5
2. 相似法（复合滑移部分） ……18

行业先锋

1. 浦林成山（山东）轮胎有限公司研发实力简介 ……24
2. 苏州同元系统建模仿真软件及其在轮胎动力学仿真中应用 ……27
3. 青岛森麒麟轮胎股份有限公司研发实力简介 ……30

快讯精选

1. 2019轮胎与车辆动力学院士论坛盛大召开 ……34
2. 第三届理事会暨轮胎与车辆动力学技术论坛成功召开 ……38
3. 轮学盟2020年会议计划 ……42

卷首语

夯实行业创新发展的的基础技术----轮胎动力学

郭孔辉

著名汽车设计研究专家，中国工程院院士，吉林大学汽车学科带头人、教授、博士生导师。

郭院士在汽车系统动力学及其相关领域造诣精深。在轮胎力学、汽车动力学以及人—车闭环操纵动力学等方面的研究成果均达到世界先进水平。是最早把近代系统力学与随机振动引入汽车科学研究的学者。在汽车振动与载荷方面，系统的、具有开创性的著述在国内外都有重要的影响。也是我国汽车科学技术领域中汽车操纵稳定性、平顺性、制动与驱动稳定性及轮胎力学等领域的主要开拓者和学术带头人，为我国汽车工业科学技术的发展做出了重要的贡献。

轮学盟的这一期《轮胎动力学通讯》刚好是 2019 年的最后一期，正值岁末年初之际。回望这一年，轮胎、汽车业可以用“雄关漫道真如铁”来形容，经济下行、政策变化、融资困难对行业都有着不小的冲击。面对如此严峻的局面，不少企业提出要进行技术创新，提升科研实力以应对难关。事实的确如此，科研是引领发展的第一动力。对于整车开发来说，科研的基础就是车辆动力学，而轮胎动力学更被誉为车辆动力学皇冠上的明珠，是高性能汽车开发的基础理论及关键技术。

我国轮胎动力学的研究从上世纪 60 年代红旗轿车高速稳定性出现问题开始，由 1984 年成功开发 QY7329 轮胎试验台而得以快速推进。发展至今，轮胎动力学的研究从稳态到非稳态，从线性到非线性，模型已经相当丰富。先进车辆底盘控制系统的设计与分析、车辆系统结构和零部件的优化设计，都是建立在轮胎动力学特性研究基础上的。

近几年，人工智能、云计算、大数据、5G 纷纷进入汽车行业，行业中不少企业都在做智能网联车辆。我的一些研究生也和我说，想要做智能车，但是我对他们的回答往往是让他们先做好汽车，也就是车辆动力学、轮胎动力学这些基础技术，搭建模型对于整车开发非常重要。如果基础都无法夯实，又何以谈论进一步的提升呢。

绝大部分企业已经充分认识到轮胎动力学性能研究的重要性，投入了不少人力、物力并取得了一些成效，但是我们仍需要承认，对于整个行业来说，轮胎动力学依然是我们的短板。关键共性技术攻关、相关标准法规缺失、产业上下游缺乏诉求沟通等等，这些都是我们亟待解决的问题。在这方面，轮胎动力学协同创新联盟的创建与发展就有着非比寻常的意义。成立以来，联盟已带领众多会员单位在突破关键共性技术、整合对接国际资源、完善标准法规体系、提升

测试评价能力方面做出了一定成绩，希望联盟在今后得到更好的发展，成为行业的“领头羊”，共同探索出应对机遇和挑战的发展之路。

无论是过去、现在，还是未来，车辆动力学与轮胎动力学在整车开发中都是不可或缺的、至关重要的一部分。而作为汽车技术发展最为活跃的区域，我国快速的技术更新提供了轮胎动力学快速发展的机遇，在此我希望轮学盟能抓住机遇，乘行业发展东风、借业界精英之力，有效推进轮胎动力学研究工作，共绘互利互助的美好蓝图！

封面故事

2019 轮学盟“外智大师班”研讨会圆满落幕

为加强国内外技术交流、吸纳先进技术，11 月 20 日，轮胎动力学协同创新联盟在上海举办 2019 年“外智大师班”研讨会。本次会议为轮学盟举办的轮胎与车辆动力学精品会议，邀请到日本工学院大学中岛教授和曾在美国通用汽车公司有 20 年工作经验的吴博士作为授课老师，共 36 位与会专家。11 月 20-21 日，由中岛教授授课；11 月 22-23 日，由吴博士授课。

20 日，由中岛教授开始“外智大师班”第一课。会议中，中岛教授为大家讲解“复合材料力学与结构设计”及“轮胎轮廓力学(胎侧与胎冠)”，其中，复合材料力学与结构设计包括单层复合材料力学、经典薄板理论、修正薄板理论、离散薄板理论、有限元法等内容；轮胎轮廓力学(胎侧与胎冠)主要包括胎侧轮廓理论、非自然平衡轮廓性能控制思想等内容。21 日，中岛教授为参会专家讲解“轮胎花纹力学”和“未来轮胎技术”，其中，“轮胎花纹力学”主要包括胎面花纹刚度、胎面花纹噪声、节距排列、滑水、雪地牵引、花纹沟排水、PRAT 等内容；“未来轮胎技术”主要包括轮胎环境、未来的轮胎力学:可持续性技术、非充气轮胎未来技术、智能轮胎未来技术等内容，为与会专家描绘出未来的轮胎技术蓝图。

11 月 22 日起，由吴旭亭博士担任授课老师。22 日，吴博士讲解《乘用车和轻型卡车底盘开发与车辆动力学基础》。吴博士从底盘开发与车辆动力学发展简史、车辆动力学覆盖的范围及重要性讲起，逐步过渡到整车集成与悬架转向系统、整车动力学性能简介、整车架构参数与车辆动力学性能、车辆动力学在底盘开发中的作用、底盘开发中的工具、底盘开发流程等多方面。23 日，吴博士为大家讲解《乘用车和轻型卡车车辆操纵稳定性与控制》，本课程是 22 日课程《乘用车和轻型卡车底盘开发与车辆动力学基础》在车辆操纵稳定性能方面的延伸，详细介绍了横摆稳定性和侧翻稳定性、转向性能以及相应的控制系统。讲解过程中，吴博士以其幽默风趣的语言，深入浅出地向大家展示了其多年来所积淀的汽车底盘开发和车辆动力学实践经验。

图 1 中岛幸雄教授

图 2 吴旭亭博士

会议结束后，吴博士为与会专家颁发本次会议结业证书。

对于中岛教授的授课内容，参会专家表示受益良多，山东玲珑轮胎股份有限公司路波部长说道，“感谢中岛教授用深厚的基础理论知识和丰富的经验带来这次课程，印象深刻的是轮胎通过复合材料受力分析支撑所有的轮胎性能分析，理论充分，逻辑清晰。还有花纹分析，通过模型和 FEA 技术开发，理解了轮胎花纹各种性能的机理。这让我们对于问题的研究有新的认识和思路。”

针对吴博士的讲解，中国第一汽车集团公司研发总院工程师吕满意说道，“吴博士的工程经验非常丰富，对车辆动力学的历史和发展历程如数家珍，讲课风格风趣幽默，深入浅出，旁征博引，分别从设计、试验、仿真、调校等角度详细介绍了车辆动力学及其与整车和其他性能的关系，并指出车辆动力学并不只是底盘的特性，而是应该上升到整车的高度，积极参与并指导整车设计。这些都帮助我们更深刻地理解车辆动力学。希望在以后的工作中可以和吴博士更多地交流！”

轮学盟 2018 年提出了“走出去，引进来”的方针，经过不断探索，于 2019 年首次尝试以“外智大师班”的形式将国外先进技术“引进来”。轮学盟将总结本次会议经验，逐步将“外智大师班”打造成国内轮胎与车辆动力学品牌课程。2020 年轮学盟计划开展两次“外智大师班”研讨会，加强国际交流，引进更多国际先进技术,在一定程度上提高国内轮胎、汽车底盘开发实力。

图 3 与会专家与中岛教授合影

图 4 与会专家与吴旭亭博士合影

技术前沿

Parameter Identification and Validation for Combined Slip Tire Models using a Vehicle Measurement System

Matthew Van Gennip[1]

1 A&D Technology Trading (Shanghai)Co., Ltd.

Abstract

It is imperative to have accurate tire models when trying to control the trajectory of a vehicle. With the emergence of autonomous vehicles, it is more important than ever before to have models that predict how the vehicle will operate in any situation. Many different types of tire models have been developed and validated, including physics based models such as brush models, black box models, finite element based models, and empirical models driven by data such as the Magic Formula model. The latter is widely acknowledged to be one of the most accurate tire models available; however collecting data for this model is not an easy task. Collecting data is often accomplished through rigorous testing in a dedicated facility. This is a long and expensive procedure which generally destroys many tires before a comprehensive dataset is acquired. Using a Vehicle Measurement System (VMS), tires can be modeled through on-road data alone. This reduces the time and cost significantly, and does not require destroying multiple tires. Previous works regarding this parameter identification method have used only the basic versions of the Magic Formula model – pure longitudinal slip and lateral sideslip – but the Magic Formula model also includes combined slip conditions as well. To accurately mimic the tire forces, especially in safety critical situations for autonomous vehicles, combined slip tire models are necessary. The longitudinal slip, side slip angle, tire forces, and tire moments are measured and calculated using a VMS during normal and extreme driving scenarios. The data is then used to identify the parameters for the 1989 Pacejka model for both pure slip and combined slip scenarios. These models are then implemented and validated with a full vehicle dynamic model.

Introduction

Autonomous vehicles are getting much attention these days.[1, 2, 3, 4] There are many different aspects to a driverless vehicle, including path planning [1], image processing [2-4], data analysis, and the low level control of the vehicle [5]. All these processes are important; they need to work in tandem for the vehicle to be able to drive itself. Regardless of how good all the components are, the vehicle itself must be able to follow the desired trajectory. This can be accomplished by using an accurate vehicle dynamic model to assess the safety and feasibility of a given trajectory [6].

Accurate tire-force models are vital components in vehicle modeling in order to analyze and simulate a vehicle trajectory [7]. These models dictate how much longitudinal and lateral force are available for each tire. Based on this information, the vehicle controller can determine what inputs are needed in order for the vehicle to follow a reference trajectory [8]. An important aspect of tire modeling is the effect of tire forces in both the longitudinal and lateral directions simultaneously. This is vital information since generally both forces will be required to follow the given trajectory, or to determine if the reference trajectory is even possible.

Tires are one of the most difficult parts of a vehicle to model accurately. Over the years, many different models have been developed that provide varying accuracy. These include linear tire models [9], physics based models such as the Brush model [10], the flexible model [11], and the Dugoff model [12-13], black box models [14-15], finite element based models [16-18], and data-driven empirical models [19]. For many situations the simplicity and ease of linear tire models is sufficient for the task; however other tasks may require a more accurate model. For a complicated task such as controlling the trajectory of an autonomous vehicle, these models are vital to ensure the vehicle controller does the best possible job. Normally these models are developed in dedicated test facilities that can run controlled tests on the vehicle tires. Unfortunately, these tests are expensive and time consuming while resulting in models that may not be accurate enough under real road conditions. One of the main limitations of testing in test rigs is that any data outside the measurement range can only be extrapolated as approximations. Another major limitation is that the rolling belts or drums may not be representative of real roads. As such, on-road measurements may lead to better practical results even though there is less control available during testing.

There are some downsides and limitations to developing tire models using on-road data alone. The main limitations is the ability to control the conditions of the tests. When performing tire tests on a rig, all the parameters and conditions of the test can be set and accurately reproduced. Unlike rig testing, road testing results will vary depending on many uncontrollable parameters such as pavement conditions, tire temperature, and wind conditions. Due to this, the repeatability of the tests can sometimes be an issue; however this can be mitigated by measuring certain external variables

such as the temperature, wind speed, and friction coefficient of the road. By measuring these values, their variability can be accounted for during data analysis. Details regarding test repeatability are discussed in the Testing section.

Another limitation of on-road testing is the ability to measure specific data points. For instance, it is difficult to measure data with both a large positive longitudinal slip value along with a large sideslip value. In cases like this, it may be that the vehicle is unable to achieve these values due to mechanical limitations. In these situations it is acceptable to not have data since the vehicle will never encounter such a scenario. In other cases it may be difficult to cause the vehicle to perform the necessary maneuver in order to collect the desired data. These cases have been taken into consideration when developing the testing to be performed on the vehicle.

This article develops pure and combined slip 1989 Pacejka tire models for an autonomous 2015 Hybrid Lincoln MKZ using on-road data alone from a Vehicle Measurement System (VMS) by A&D Technology [19]. The article presents a method for quickly developing an accurate tire model to be used in vehicle simulation and controller development.

There has been previous work using the VMS for vehicle parameter identification; however it has been limited to longitudinal dynamics [6], [7]. Consequentially, all tire models that have been developed using the VMS have been limited to longitudinal Pacejka models. This article delves into lateral dynamics and identifies the parameters for the lateral Pacejka model along with the various parameters during combined slip conditions, when both longitudinal and lateral forces are acting upon the wheel simultaneously.

This article first covers the modelling methodology and literature review, followed by an overview of the technology used to gather a comprehensive data set. Next, the various tests performed are outlined in detail. Following this, the results are presented, including the tire models for pure longitudinal slip conditions, pure lateral slip conditions, and combined slip conditions. Lastly, there is a brief discussion of the results, ending in the conclusion.

Tire Modelling and Literature Review

This section covers the basics of tire modeling, including a brief literature review and explanation of both the linear tire model and the Pacejka model. This article uses the SAE tire axis system [24].

Tire modeling is primarily used for determining the longitudinal (tractive) and lateral forces exerted by a tire, specifically when the vehicle is in motion. The tractive force is mainly dependent on longitudinal slip. Longitudinal slip is defined as follows [24]:

$$s = \frac{(v - r\omega)}{v} \tag{1}$$

Where s is the longitudinal slip, v is the velocity of the vehicle at the venter of the tire, r is the radius of the wheel, and ω is the angular velocity of the wheel. The longitudinal slip is generally very small, however even slight differences in longitudinal slip can have drastic effects on the tractive force.

The lateral force is mainly dependent on the sideslip angle of the tire. Sideslip is defined as the angle between the wheel heading and the direction of motion [24]. Just like longitudinal slip, this value is generally very small, normally less than four degrees; however these small changes also have drastic effects on the lateral force.

Both the longitudinal force and lateral force are also dependent on the normal load of the tire, which itself is dependent on many variables such as the static weight of the test vehicle, the grade of the road, the location of the center of gravity, along with any acceleration, pitch, and roll encountered by the vehicle. During an on-road maneuver, the normal load on each tire will vary greatly. This constitutes one main benefit for testing on a dedicated test rig, since the normal load on the tire can be provided as an input. To account for the changing normal load during on-road testing, the longitudinal and lateral forces must be normalized. Details about this procedure can be found in the Results section.

Both the longitudinal and lateral forces on the tire are developed through a generalized simplification of the tire patch dynamics. As the camber angle of the tire increases, the contact patch will deform, causing changes in the observed forces. The increase in camber angle will cause a camber thrust force [26], which generally adds to the observed lateral forces. Camber thrust can be taken to be directly proportional to the camber angle [27]. Details regarding how camber thrust is accounted for can be seen in the Results section.

There are other additional factors that affect the observed forces on the tire, such as the friction coefficient of the road, the tire temperature, and the tread wear. The tire tread will degrade over extended and extreme use. As the tread degrades, the available forces will decrease. This effect is not considered in this paper since the application is for normal driving scenarios with tires in good condition. The temperature of the tire also impacts the longitudinal and lateral forces. Since the vehicle will be used for normal driving scenarios, the change in temperature is neglected since the corresponding change in forces is insignificant.

Lastly, the friction coefficient of the road determines how much force is available for the tires. Driving on dry pavement as opposed to ice is extremely different due to the difference in the friction coefficient. In this paper the friction coefficient is assumed to be constant. For simulation purposes this is acceptable since the friction coefficient is provided as an input; however if these models are used on a vehicle controller, there will need to be an estimator in order to identify the friction coefficient.

A number of tire models have been developed for use with on-road measurement data as opposed to data gathered from a test rig. One of these models is the Thermal and Mechanical tire model (TAME) [20-21]. This model is an accurate representation of a vehicle tire, even more accurate than the Pacejka tire model due to the inclusion of thermal properties. Consequentially, this model is useful for extreme driving situations, such as racing, whereas it is less important during normal driving scenarios, where the thermal properties of the tire do not vary greatly. Since the intended application is to be used for normal everyday driving, this model is not used since the added complexity of this model is not required.

A much simpler tire model is a linear tire model [23]. As the name suggests, this model varies linearly with longitudinal slip and sideslip angle. The formulas for this model are outlined in Equations 2 through 3.

$$F_x(s) = C_x s\, F_z \tag{2}$$

$$F_y(\alpha) = C_y \alpha\, F_z \tag{3}$$

Where s is the longitudinal slip, α is the sideslip of the wheel, C_x is the longitudinal stiffness of the tire, and C_y is the cornering stiffness of the tire. This model is useful since it is easy to implement due to the simplicity of the equations, however it is only accurate for very low longitudinal slip and sideslip angle values. Normal driving situations may exceed these limits, causing the model to become inaccurate.

The Pacejka tire model is a far more accurate representation of the tire forces. There are many different versions of the Pacejka model, the most recent version being in 2012 – PAC 2012 [1]. Each revision of the model adds more accuracy and complexity; adding properties to include combined slip conditions, advanced tire-transient behaviors, and other factors. In order to increase accuracy beyond the simple linear tire model, while also not increasing the complexity too much, the 1989 Pacejka tire model is used. The formulas for the 1989 version of are outlined below in Equations 4 through 5. This model depends on both the longitudinal slip/sideslip angle and the normal force on the tire.

$$F_x(s,F_z) = D \sin\left(C \tan^{-1}\left(Bs - E\left(Bs - \tan^{-1}(Bs)\right)\right)\right) F_z \tag{4}$$

$$F_y(\alpha,F_z) = D \sin\left(C \tan^{-1}\left(B\alpha - E\left(B\alpha - \tan^{-1}(B\alpha)\right)\right)\right) F_z \tag{5}$$

Where B, C, D, and E are all constants. These complicated formulas are still a simple model compared with more recent versions of the Pacejka tire model [1]. It is worth noting that these models only work under pure slip conditions. That is to say that these models only work when either a longitudinal force is being applied or a lateral force is being applied, not when both are applied simultaneously. To account for this condition, called combined slip, an updated Pacejka model, such as PAC 2012, could be used. This solution is not used in this paper due to the large number of parameters involved, which detracts from the objective of creating a simple, accurate tire model. Instead, a piecewise combined slip model is used. This model captures the tire forces and moments under combined slip scenarios, resulting in improved accuracy over the pure slip models while maintaining the relative simplicity of the 1989 Pacejka tire model.

This paper does not develop a new model; instead the parameter identification for the 1989 Pacejka tire model is shown for various combined slip scenarios. This model is for one ambient temperature and one road friction coefficient. Additional parameter identification is needed in order to develop tire models at other conditions.

Data Collection

One of the main issues with the Pacejka model is collecting a comprehensive dataset. Collecting data is often accomplished through rigorous testing in a dedicated facility. This is a long and expensive procedure that will generally destroy many tires before enough data is acquired. Using the Vehicle Measurement System (VMS) by A&D Technology [19], combined slip Pacejka tire models can be quickly developed through on-road data alone. This reduces the time and cost significantly and does not require destroying multiple tires.

The VMS consists of three main sensor modules which are attached to each of the four wheels. These sensor modules are the Wheel Force Sensor (WFS), Wheel Position Sensor (WPS), and Laser Ground Sensor/Laser Doppler Velocimeter (LGS/LDV). Each sensor module collects a variety of signals detailed below. All data signals are recorded at a rate of 100Hz.

The WFS consists of a custom wheel hub comprised of strain gauges. These strain gauges measure the longitudinal, lateral, and normal force

on each wheel. They also measure each of the moments about the above axis. In addition to these measurements there is also a sensor which measures the angular velocity of the wheel and the average temperature of the tire. All of these measurements are taken at the center of the wheel.

The WPS is a large truss system that consists of five digital encoders which determine the X-Y-Z location of the wheel relative to the chassis along with the camber and toe angles of the wheel.

The LGS/LDV consists of five laser sensors. Two of these sensors measure the longitudinal and lateral speed of the vehicle at the tire. The other three sensors measure the current ride height of the vehicle which is useful for determining the effective wheel radius throughout the test. Figure 1 shows one wheel of the test vehicle – 2015 Hybrid Electric Lincoln MKZ – with the VMS attached to it.

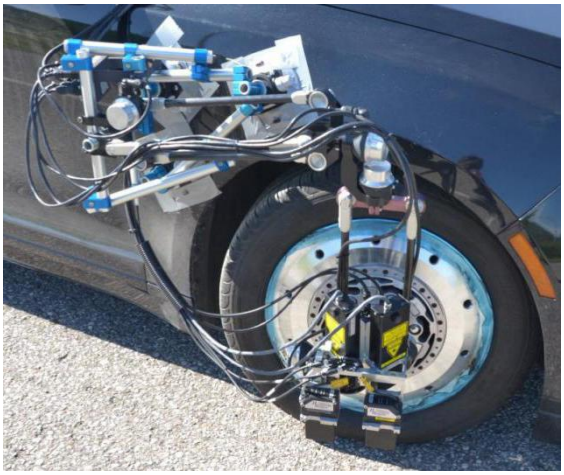

Figure 1: The VMS Attached to a Wheel

In addition to the VMS, data was collected from a Racelogic VBOX3i, which contains an Inertia Measurement Unit (IMU) and a Global Positioning System (GPS). These values are not used in the development of the tire model; they are only used for model validation.

Testing

To get a comprehensive data set, a number of tests must be performed. Each test is performed a minimum of four times in order to eliminate potentially erroneous data.

To collect data for the pure longitudinal slip model, a rapid acceleration and braking test is performed. The vehicle is accelerated quickly from rest to a speed of 100km/h, after which the brakes are applied, returning to rest as quickly as possible. A lower top speed can be used if necessary. The most important part of this test is the quick transients, which will excite large longitudinal slip, filling in most of the nonlinear data regions. This single test is able to provide sufficient data for the pure longitudinal slip Pacejka model.

As opposed to the single test needed for the longitudinal model, three different tests are performed to obtain a sufficiently rich dataset for the pure lateral slip model. First, a steady state cornering test is performed. This test involves driving in a circle with a constant radius at a constant speed. This test is performed according to ISO standards [ISO 4138:2012] with a radius of 15m, 20m, and 25m. The second test is a double lane change maneuver. In this test the vehicle travels at a constant speed through a typical double lane change motion. This test is also performed according to ISO standards [ISO 3888-1:1999] at speeds of 60km/h, 80km/h, and 100km/h. The last test is a step steer test. This test involves traveling in a straight line at a constant speed and then suddenly applying a large steer input. This is also done according to ISO standards [ISO 7401:2011] at speeds of 50km/h, 60km/h, and 70km/h with an approximate 120deg, 90deg, and 60deg steer angle input respectively. Before attempting the step steer test, multiple dry runs were executed to determine a safe steering angle at each of the above speeds.

It can be difficult to obtain data for pure longitudinal and pure lateral slip models using on-road data. This is simply because of the lack of control available during the road tests. For the above tests, the gathered data contained combined slip data points as it is practically impossible to encounter zero longitudinal or lateral force, however this was accounted for. For the pure longitudinal slip test it is relatively easy to ensure only small lateral forces are observed by simply keeping the steering wheel straight. Throughout this test there is a small constant sideslip angle caused from the toe angle, necessary for vehicle controllability; however any data points with larger sideslip values are ignored for the pure longitudinal slip analysis. Likewise, for the pure lateral slip tests, any data points with large longitudinal slip values are disregarded during the analysis. Maintaining small longitudinal slip values throughout the lateral tests is more difficult, but with the large variety of tests performed, a comprehensive data set is gathered nonetheless.

For the combined slip Pacejka model, two tests are performed to obtain the necessary data. First, a modified step steer test is performed. The only difference from the above test procedure is that after the steering angle is applied, a large braking force is also applied. This results in data that has both a large longitudinal slip and a large side-slip angle. This test is only able to gather data for the negative longitudinal slip (braking) region since it is difficult to achieve large positive longitudinal slip during this maneuver. This is due to the mechanical limitations of the vehicle. The second test that is performed is dubbed the grand sweep maneuver. In this test, the

steering wheel angle changes at a constant rate in either the clockwise or counterclockwise direction according to the following criteria. The speed of the vehicle is not to exceed 70km/h and not to fall below 30km/h. While increasing the steer angle in either direction past the neutral straight wheel state (a steering angle of zero degrees), the brakes are applied. The braking should be tuned so as to slow down the vehicle from the approximate speeds of 70km/h to 30km/h by the time the steering wheel angle rotates a full 360 degrees. While the steer angle is decreasing back to the neutral straight wheel state, the accelerator pedal is applied. The acceleration should be tuned so as to speed up the vehicle from the approximate speeds of 30km/h to 70km/h by the time the steering wheel angle returns to zero degrees – the neutral straight wheel state. Once the steering angle is back to zero degrees, the wheel should continue to rotate in the same direction – so as to turn in the other direction – with the above criteria in mind. This process is repeated a total of ten times. Ultimately this maneuver results in the vehicle traveling in a figure eight pattern. Like the previous test, it is more difficult to excite large positive longitudinal slip than it is to excite large negative longitudinal slip; a powerful engine would be needed in order to excite this region.

Many tests had to be tweaked and repeated to improve repeatability while still obtaining a sufficiently rich data set. Even though the exact inputs for each maneuver are difficult to reproduce, by following the details above, the resulting data is nearly identical each time the test is repeated. The above maneuvers were repeated a minimum of five times, and for each maneuver except the grand sweep maneuver it was found that for each value of longitudinal slip or lateral sideslip, the recorded normalized force had a maximum standard deviation of 0.0802. The grand sweep maneuver was more difficult to repeat due to the complexity of the maneuver, having a standard deviation of 0.118.

All of the tests detailed above are the final versions; easily repeatable with the exception of the grand sweep maneuver. All of the pure lateral slip tests are according to ISO standards, and the desired trajectories were outlined with traffic pylons to ensure the tests adhered to these standards.

Results

Before using the data collected from the tests, the data must be quickly analyzed to ensure it is valid. Through a simple visual analysis of various data signals, it can be seen that the collected data is reasonable. A plot overlaying the wheel speed (angular velocity multiplied by effective wheel radius) and the measured vehicle speed is shown in Figure 2. As seen, these values follow the same approximate curve. The small differences are due to the longitudinal tire slip. Figure 3 shows the tractive and normal forces for the same maneuver, which also act in a sensible manner. These two plots support the validity of the experimental data.

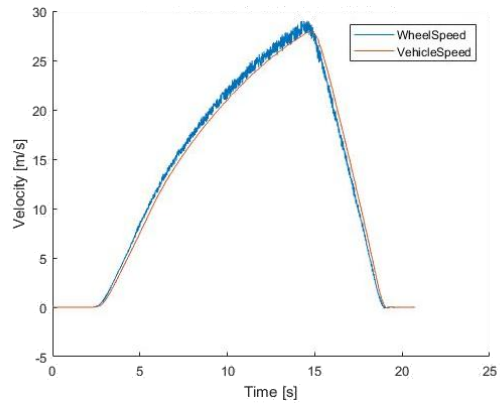

Figure 2: Wheel Speed and Vehicle Speed for the Pure Longitudinal Slip Test

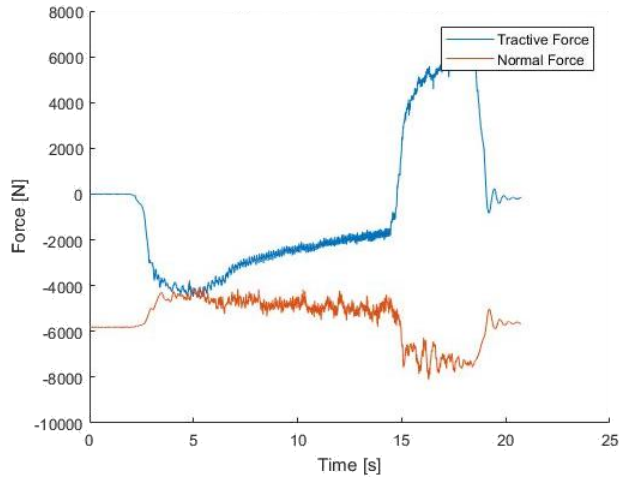

Figure 3: Wheel Tractive and Normal Forces for the Pure Longitudinal Slip Test

The plots above simply show the raw output data from the VMS. To use the data for tire modeling, some processing must be done. Primarily the sideslip angle and longitudinal slip ratio must be calculated.

Longitudinal slip, defined in Equation 1, is calculated by dividing by the vehicle speed. Consequentially, all test points where the vehicle speed is zero will cause a singularity. These data points must be removed. The sideslip angle is calculated by observing the longitudinal and lateral speed of the tire, measured by the LGS/LDV. If there is no lateral speed, then the tire heading is the same as the tire direction of motion, meaning the sideslip angle is zero. If lateral speeds are observed then the resultant direction of motion is found using the Pythagorean theorem. A simple trigonometric identity gives the sideslip angle of the tire. This is outlined in Equation 6.

$$\alpha = \tan^{-1}\left(\frac{Lateral\,Speed}{Longitudinal\,Speed}\right) \qquad (6)$$

As described earlier, the tire forces depend upon

the normal load experienced by the tire. As shown in Figure 3, the normal load on the tire is measured and accounted for in the model. This is done by dividing the recorded longitudinal and lateral forces by the normal load. This normalization accounts for all the changes in tire behavior due to normal load. The normalized longitudinal Pacejka tire model is shown in Equation 7.

$$\frac{F_x}{F_z}(s) = D\sin\left(C\tan^{-1}\left(Bs - E(Bs - \tan^{-1}(Bs))\right)\right) \tag{7}$$

Some post processing must also be done using measurements from the WPS. During more extreme testing maneuvers, the camber angle of the tires increase. The reference frame of the WFS is fixed to the wheel. Based on this, as the camber angle increases, part of the normal load is actually measured as a lateral force, and vice versa. The camber angle is measured using the WPS and used to apply a coordinate transformation to the measured forces from the WPS to ensure that the normal loads are normal to the road. Through this process the camber thrust is accounted for.

Lastly, since the tire forces are measured at the center of the wheel hub, post processing is done to determine the forces at the tire contact patch itself. First, a simple coordinate transformation is necessary in order to identify the forces at the contact patch itself. In addition, an inertial force is observed due to the WFS, the wheel, and the tire itself. This force is easily removed from the measured data using the measured weights of the components.

Pure Longitudinal Slip Pacejka Model

The normalized pure longitudinal slip Pacejka model, detailed in Equation 7, depends solely on longitudinal slip. As stated earlier, many other factors also influence the longitudinal force. Many of these factors are taken into account during data processing however many of these factors are also ignored in order to simplify the model. Figure 4 shows the processed data for the pure longitudinal slip acceleration/braking test. The x-axis is the longitudinal slip and the y-axis is the unitless normalized longitudinal force.

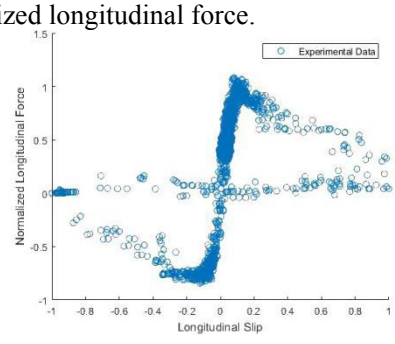

Figure 4: Measured Data from Pure Longitudinal Slip Test

It can be seen that many of these data points are erroneous. There should be no high slip values that provide a near-zero force. These data points are all erroneous values that occur when the vehicle is at a near zero speed. From the definition of longitudinal slip it can be seen that when the vehicle speed is near-zero the slip values are more prone to error. Post processing removes all singularities by removing all data points with a vehicle speed of zero, however near zero speeds will also cause erroneous data due to the asymptote. By removing these values, a more representative data set is obtained.

Using this data set, a nonlinear least squares optimizing routine is performed to identify the Pacejka parameters in Equation 7. This was done using the Matlab Curve Fitting toolbox. The parameters for this Pacejka tire model are provided in the Appendix. The resulting Pacejka curve is shown with the experimental data set in Figure 5. In addition, a linear tire model is also fit to show a comparison between these two models.

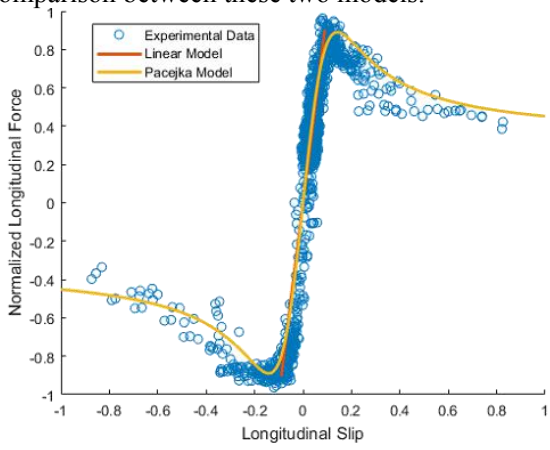

Figure 5: Pure Longitudinal Slip vs. Normalized Longitudinal Force

The linear tire model shown in Figure 5 is accurate for small values of longitudinal slip. The linear tire model is much simpler than the Pacejka model; however the use of the linear tire model is limited. Likewise, the pure longitudinal slip 1989 Pacejka tire model is much simpler than other tire models; however it has limited use.

The pure longitudinal slip Pacejka model was developed using data points from every run for the test specified in the previous section. It is worth noting that when performing the optimization for only the data points for each individual run, the resulting parameters only differ by a maximum of 1.8%. This helps validate the repeatability of the designed test.

Pure Lateral Slip Pacejka Model

The pure lateral slip model is determined in a similar fashion as the pure longitudinal slip, however instead of longitudinal slip, the sideslip angle is used. Sideslip is defined as the angle between the heading

of the wheel and the instantaneous direction of motion. Details for calculating the sideslip angle based on experimental data is found near the beginning of the Results section. Like the longitudinal model, the lateral tire force is divided through by the normal load in order to calculate the normalized lateral force. By normalizing the lateral force, the change in lateral force due to the normal load is accounted for.

Like the pure longitudinal slip model, there will be a number of erroneous data points while the vehicle is near zero speed. This is due to the calculation of the sideslip angle; calculated by dividing by the longitudinal speed of the wheel. After removing the erroneous data while the vehicle was near zero speed and combining the data from each of the three different tests performed, a comprehensive data set is achieved. The data points are plotted Figure 6. Once again a simple optimization is run in order to determine the Pacejka curve parameters necessary for the model to fit the data. The parameters for this curve are shown in the Appendix.

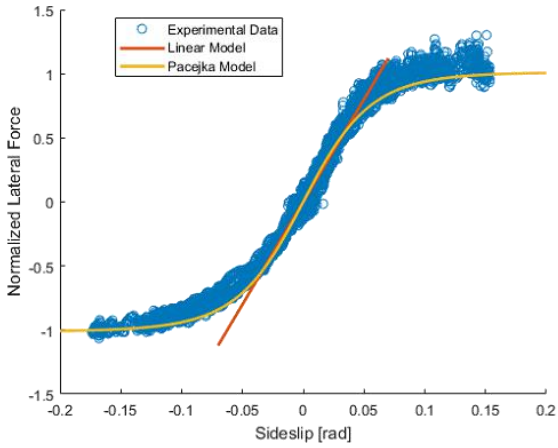

Figure 6: Pure Sideslip vs. Normalized Lateral Force

It is worth noting that the experimental data points shown in Figure 6 have a higher standard deviation than the longitudinal results in Figure 5. This is seen as the thickness of the experimental curve. The standard deviation is larger due to multiple reasons. Primarily it is due to many of the simplifications that were used for this model, such as neglecting camber thrust and temperature changes. It was observed that the tire temperature varied more during the lateral tests than during the longitudinal test.

The increased standard deviation is also likely due to the normalization process. The normal load observed on the tires vary more during the lateral tests as opposed to the longitudinal tests. These transients increase the standard deviation slightly.

Combined Slip Pacejka Model

The combined slip model is far more complicated than either of the longitudinal or lateral models due to the effects of the friction ellipse [14]. The friction ellipse is based on the Equation 8:

$$\frac{F_x^2}{\mu_x^2} + \frac{F_y^2}{\mu_y^2} = F_z{}^2 \tag{8}$$

A visual representation of the friction ellipse is shown in Figure 7.

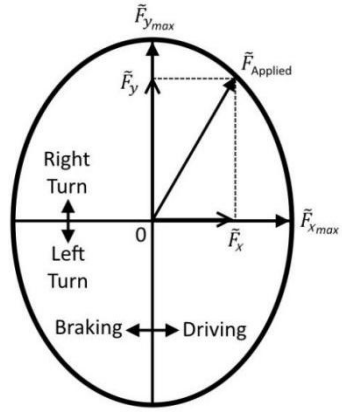

Figure 7: Visualization of the Friction Ellipse

Basically, there is a maximum amount of force available to be applied by the tire. If force is only applied in the longitudinal direction, pure longitudinal slip, then the maximum available force is $\tilde{F}_{x_{max}}$. Likewise, if force is only applied in the lateral direction, pure lateral slip, then the maximum available force is $\tilde{F}_{y_{max}}$. The problem arises when both longitudinal and lateral forces are encountered at the same time. When force is applied in both the longitudinal and lateral directions, the maximum available force is shown as $\tilde{F}_{Applied}$; however the longitudinal and lateral components of this force are less than $\tilde{F}_{x_{max}}$ and $\tilde{F}_{x_{max}}$.

Under normal driving situations, this effect is not prevalent due to a very small necessary lateral force. The purpose of developing these models is to implement them on an autonomous vehicle. Most maneuvers the vehicle will perform are normal driving situations where this effect is not substantial; however in a safety-critical situation where an autonomous vehicle must try to avoid an obstacle, this reduced maximum force is vital information.

Because of this, a combined slip model is developed. The following work is completed for both the longitudinal and lateral combined slip models; however since the process for both of these models is identical, only the longitudinal work will be presented. The data gathered through the two combined slip tests are compiled together and any erroneous data is removed, just as it was in the pure slip models. To determine if there is actually a large effect on available forces during combined slip conditions, the normalized longitudinal force was plotted against the normalized lateral force. The resulting plot is cluttered due to the sheer number of data points. As such, many of the data points were

trimmed only for visualization, shown in Figure 8.

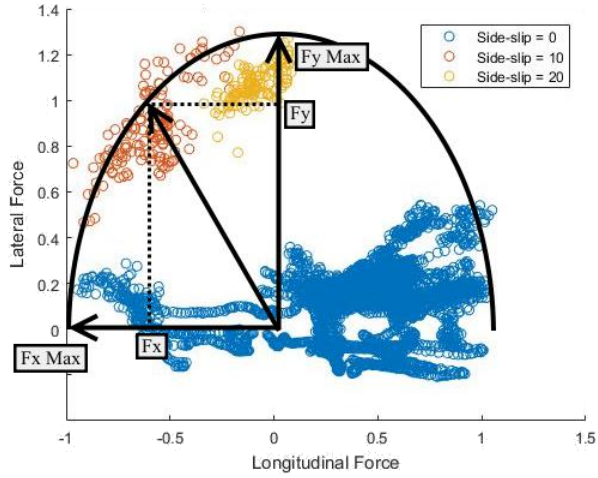

Figure 8: Normalized Longitudinal Force vs. Normalized Lateral Force

It is worth noting that every point inside the friction ellipse is a feasible point. The tires do not need to apply the maximum available force, rather they are limited by the maximum force. This is why many of the data points in Figure 8 are arrayed inside the border of the ellipse. As the sideslip values increase, the longitudinal force observed decreases while the lateral force increases. Only a few of the data points for larger sideslip values are shown; however it is easy to see that as the lateral force increases the available longitudinal force decreases. It is important to note that the high lateral force values only occur during high sideslip values as expected. The low lateral forces shown for near zero sideslip values are necessary for vehicle stability.

From Figure 8 it is seen that as the absolute value of the lateral force increases, the longitudinal force decreases. Consequentially, the longitudinal slip was plotted against the normalized longitudinal force to determine the differences in the longitudinal Pacejka model. This can be seen in Figure 9. By adding a third dimension for the sideslip (different colors), it is easy to see the impact it has on the available longitudinal force.

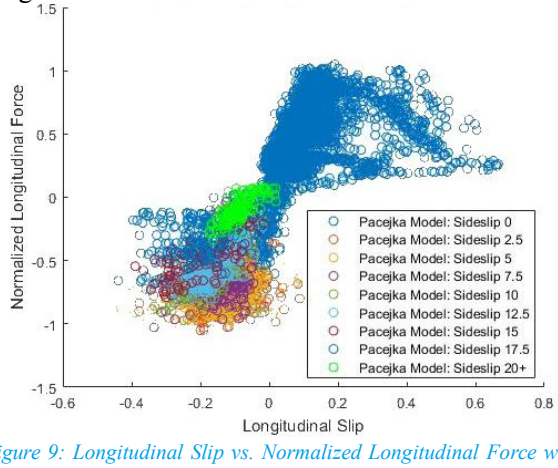

Figure 9: Longitudinal Slip vs. Normalized Longitudinal Force with Varying Sideslip

The must substantial change is seen when observing the data points with a sideslip angle of twenty degrees. It is clear that if a linear tire model was optimized around these data points, as opposed to the near zero sideslip data points, the slop of the model would be significantly different. This is the main impact that needs to be captured by the combined slip tire model.

It is important to note that large sideslip values are only shown in the negative longitudinal slip (braking) range. The sideslip values observed in the positive longitudinal slip range are ignored only for visualization purposes; they are included in calculations. In addition, it is worth noting that sideslip values exceeding 15 degrees are only seen in the braking region. This is expected, due to mechanical limitations, and was outlined in the Testing section. Fortunately the combined slip models will mainly be used in safety critical situations, when the only objective is avoiding an obstacle. During these types of situations it is likely that the vehicle will attempt to steer away from the obstacle while braking, not accelerating. Consequentially, the combined slip models are optimized more for the braking region than the accelerating region.

To create a combined slip model, a continuous function is needed to account for the change in longitudinal forces due to lateral forces and vice versa. This is accomplished by creating a piecewise function and then creating a spline to link the identified data points.

Using specific data points, multiple Pacejka curves were optimized around the different sideslip values. Curves were optimized for sideslip values of 0 (pure longitudinal slip), 2, 5, 10, 15, 20, and 25 degrees. The optimization process is identical to the process outlined in the pure slip models. More values can be used to increase the fidelity of the model; however we found the above values to be sufficient. Assuming symmetry of the Pacejka model, identical curves were used for each corresponding negative sideslip value. To increase the fidelity, new curves could be fitted for this negative region. The identified Pacejka parameters are presented in the Appendix along with the parameters for the lateral combined slip Pacejka curves.

Three of the resulting curves, for 0, 10, and 20 degrees sideslip angle, are shown in Figure 10. The experimental data shown in Figure 10 is the same as that in Figure 9; however the sideslip values were ignored for visualization to highlight the three different curves.

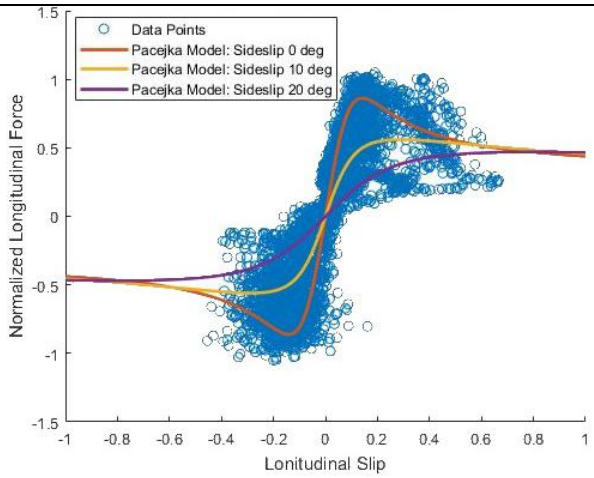

Figure 10: Combined Slip Pacejka Models for Sideslip Values of 0, 10, and 20 Degrees

As sideslip angle increases, the maximum available longitudinal force decreases significantly. This decrease is not linear in behavior, which is why the piecewise functions are necessary in order to obtain an accurate representation of the full combined slip model. Ultimately this data can be used to determine the parameters of the 2012 Pacejka model. This will eliminate the piecewise nature of the current model, however it will also require increasing the complexity of the model significantly. There are other methods that will eliminate the piecewise nature of the combined slip Pacejka model without having to identify the excessive number of parameters needed in the 2012 Pacejka model. One such method was developed by MSC Software for use in the 1989 and 1994 Pacejka models [9]. This method involves modifying the coefficient of friction values in order to change the available forces due to combined slip behavior. This is best seen by referring back to the equation for the friction ellipse, Equation 8.

By changing the coefficient of friction in both the longitudinal and lateral directions, the available forces in each of those directions will change. Referring back to Figure 8, the indicated force could be achieved by simply reducing the coefficient of friction in both directions so as to reduce the maximum forces to the indicated available forces. This method works well when only the pure slip Pacejka models are known, but since the combined slip models have also been developed here it is not necessary.

Another method for eliminating the piecewise nature of the model is to interpolate the determined values with a spline. This relates the change in slip and sideslip with the change in model parameters. This is done by interpolating each of the four Pacejka parameters individually. Using this method, the piecewise curves seen in Figure 10 reduce to a single function for longitudinal force which depends upon both longitudinal slip and sideslip angle. Likewise a lateral model is developed which also depends upon both longitudinal slip and sideslip angle. These functions are valid for all scenarios, including both pure slip and combined slip. Figure 11 shows many of the interpolated Pacejka models based on the above method.

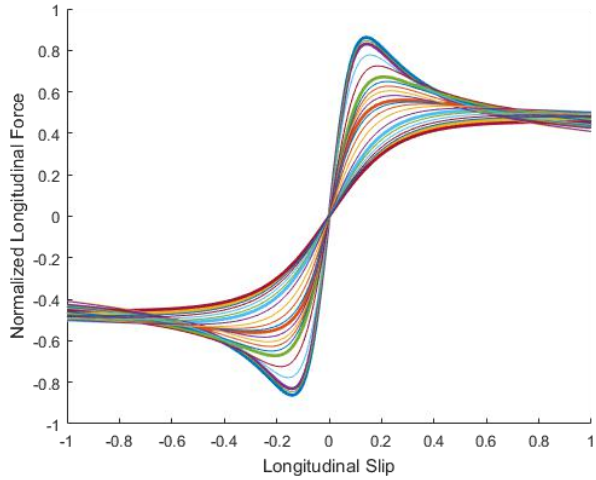

Figure 11: Results from the interpolated Combined Slip Pacejka Tire Model

This method can be used to determine accurate tire models for any combined slip scenario. Each individual tire model presented above has been created using experimental data and validated using a different set of experimental data. Once the tire models were validated, they were incorporated into a full vehicle dynamic model in order to further validate the models and test the accuracy of the different versions – linear, pure slip, and combined slip models.

Full Vehicle Dynamic Model Validation

In addition to tire modeling, a full vehicle dynamic model is developed. The vehicle is modelled using MapleSim 2017.3, a software developed by Maplesoft [25] for dynamic modeling and simulation. One advantage of this software is fast computation times since the calculations are completed through use of symbolics. The vehicle is modelled as a 14-degree of freedom multibody model. The chassis is considered to be one body with a full 6 degrees of freedom. Each tire has one degree of freedom for wheel spin. The front two wheels are also allowed to rotate about the vertical axis to model the steering of the vehicle; however these values are specified as an input steer value and therefore are not additional degrees of freedom. The last four degrees of freedom are modelled in the suspension system of the vehicle, allowing the suspension to compress and decompress. The model has five inputs: the steering wheel angle along with each of the four wheel torques. The model includes the weight of both a driver and a passenger, which were both present during experimental data

collection. The simulation is performed using a fixed step Euler solver with a step size of 0.001s.

The combined slip tire model is implemented using the interpolated spline method described in the previous section. The identified parameters are listed in the Appendix.

A random trajectory is developed to test and validate the vehicle and tire models. The trajectory performed is shown in Figure 12.

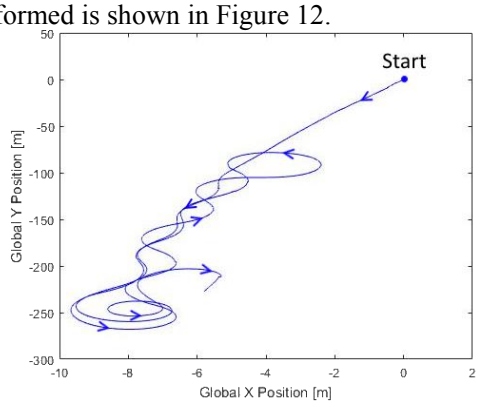

Figure 12: Trajectory of the Test Vehicle during the Validation Maneuver

Large amounts of acceleration, deceleration, and swerving are performed to encounter a variety of combined slip situations. This is done on purpose to test out the various tire models. The full vehicle dynamic model was used to compare the linear, pure slip Pacejka, and combined slip Pacejka tire models. The full vehicle dynamic model itself is not perfect; however during the following comparison, the only differences between the models are the tires themselves; all other vehicle parameters are kept constant.

To validate the model, the chassis accelerations were measured and simulated. The chassis acceleration was chosen because the intended use of these models is to simulate and control an autonomous vehicle. To accurately simulate the vehicle, the simulated accelerations should be identical to the experimental accelerations. Figure 13 shows the longitudinal acceleration versus time for the linear, pure slip, and combined slip models.

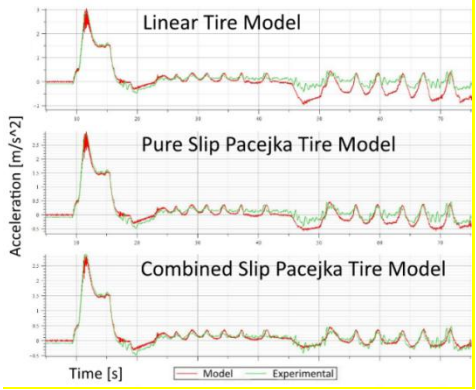

Figure 13: Full Vehicle Dynamic Longitudinal Model Validation for Three Tire Models - Linear, Pure Slip Pacejka, Combined Slip Pacejka

It can be seen that the longitudinal acceleration values at the start of the maneuver are practically identical for all of the models, with the combined slip model oscillating slightly less. As the maneuver continues however, combined slip scenarios are encountered and the models diverge. It can be seen that the pure slip Pacejka model produces better results than the linear tire models and that the combined slip Pacejka model is the most accurate of the three, as expected. Similar results can be seen when looking at the lateral acceleration of the vehicle shown in Figure 14.

It is worth noting that the model deviations occur mostly at high slip and combined slip scenarios. During these scenarios the linear and pure slip models assume that there is more force available than there actually is. Due to this, the simulated accelerations are larger than the experimental accelerations. This is the main advantage of the combined slip Pacejka tire model.

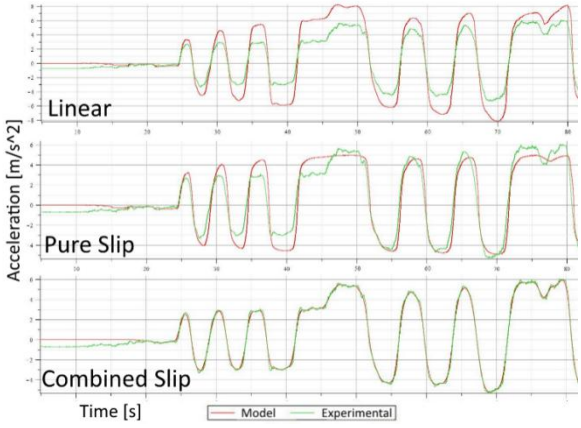

Figure 14: Full Vehicle Dynamic Lateral Model Validation for Three Tire Models - Linear, Pure Slip Pacejka, Combined Slip Pacejka

In Figure 14, it is once again seen that the pure slip Pacejka tire model estimates the forces better than the linear tire model; however it misses out on some of the characteristic behavior that is captured with the combined slip tire model. Under most circumstances this difference is small enough to not make a notable change, but in safety critical situations for an autonomous vehicle, this small difference could have a large effect on the outcome of the scenario. Consequentially it is determined that the combined slip Pacejka tire model is required in order to provide enough accuracy for autonomous vehicle applications.

Discussion

One interesting observation is that even though the Pacejka tire model is symmetric about the origin, the experimental data is slightly different for the accelerating and braking cases. This is not due to some small vertical or horizontal shift, which was found to be negligible. This is likely due to an internal braking controller used for regenerative

braking. It was found that better Pacejka models could be found by solely considering either the accelerating or braking data as opposed to the data set as a whole. This can be implemented in the piecewise combined slip model by identifying a separate set of parameters for positive and negative slip values. This change would slightly improve model accuracy however the difference is not significant.

In addition, it was found that there are slight differences between the four tires on the vehicle. These differences are generally small, likely due to varying tread wear and other issues; however a notable difference is found during cornering maneuvers between the inside wheel and the outside wheel. The difference between the inside and outside wheels vary by around 10%, which is a notable amount. This difference is likely due to the normalization process. Since the normal forces on the outside and inside tires differ by a large amount, the small error introduced through normalization is amplified, causing the observed differences to be seen. In general, this difference is ignored since the model results are accurate enough for the intended purposes.

Conclusions

A wide variety of tests were completed on the desired test vehicle to gather a comprehensive set of tire data. Using this data, the parameters for the 1989 Pacejka model were determined for pure longitudinal slip, pure lateral slip, and combined slip situations up to a maximum of 25 degrees for the sideslip angle. The added accuracy gained by this model as opposed to only using the pure slip models will increase autonomous vehicle performance in extreme scenarios. It was found that while testing the pure and combined slip models during normal driving situations, there was only a small difference between them. However, when testing these models under more extreme driving situations there was a large improvement seen through use of the combined slip model. Further tweaking and tuning of the combined slip model will result in an even larger reduction in error under similar extreme scenarios. When implemented on an autonomous vehicle, this could result in enough of a difference to avoid a potential collision. Future work involves using the determined combined slip models to determine the parameters for the PAC 2012 tire model.

References

1. Li, K., Hang, Y., Jiang, Y., He, C. et al., "A Path Planning Method Based on Large Amount of Artificial Driving Trajectories," *SAE Technical Paper* 2018-01-1588, 2018, https://doi.org/10.4271/2018-01-1588.
2. Zhong, Y., Wang, S., Xie, S., Cao, Z. et al., “3D Scene Reconstruction with Sparse LiDAR Data and Monocular Image in Single Frame,” *SAE Int. J. Passeng. Cars- Electron. Electr. Syst.* 11(1):2018, doi: 10.4271/07-11-01-0005.
3. Hu, C., Wang, Y., Yu, G., Wang, Z. et al., "Embedding CNN-Based Fast Obstacles Detection for Autonomous Vehicles," *SAE Technical Paper* 2018-01-1622, 2018, doi: 10.4271/2018-01-1622.
4. Hu, Y. and Furukawa, T., "A High-Resolution Surface Image Capture and Mapping System for Public Roads," *SAE Int. J. Passeng. Cars – Electron. Electr. Syst.* 10(2):301-309, 2017, https://doi.org/10.4271/2017-01-0082.
5. S. Bacha, M. Y. Ayad, R. Saadi, A. Aboubou, M. Bahri and M. Becherif, "Modeling and control technics for autonomous electric and hybrid vehicles path following," *2017 5th International Conference on Electrical Engineering - Boumerdes (ICEE-B)*, Boumerdes, 2017, pp. 1-12. doi: 10.1109/ICEE-B.2017.8191998
6. Sabry, Y., Aly, M., Oraby, W., and El-demerdash, S., "Fuzzy Control of Autonomous Intelligent Vehicles for Collision Avoidance Using Integrated Dynamics," *SAE Int. J. Passeng. Cars - Mech. Syst.* 11(1):5-21, 2018, https://doi.org/10.4271/06-11-01-0001.
7. Kim, C., Ludwig, C., Park, S., and IM, C., "Improvement of Tire Development Process Through Study of Tire Test Procedure and Vehicle Correlation," *SAE Technical Paper* 2018-01-1337, 2018, https://doi.org/10.4271/2018-01-1337.
8. Wu, Y., Wang, L., and Li, F., "A Robust Path Tracking Control Method for Intelligent Vehicle," *SAE Technical Paper* 2018-01-1582, 2018, https://doi.org/10.4271/2018-01-1582.
9. R. Rajamani, “Vehicle Dynamics and Control,” Springer, 2006
10. J. Svendenius and B. Wittenmark, "Brush tire model with increased flexibility," *2003 European Control Conference (ECC)*, Cambridge, UK, 2003, pp. 1863-1868. doi: 10.23919/ECC.2003.7085237
11. Yamashita H, Matsutani Y, Sugiyama H. Longitudinal Tire Dynamics Model for Transient Braking Analysis: ANCF-LuGre Tire Model. *ASME. J. Comput. Nonlinear Dynam.* 2015; 10(3): 031003-031003-11. doi:10.1115/1.4028335.
12. Ding, N., Taheri, S., “A Modified Dugoff Tire Model for Combined-slip Forces.” *Tire Science and Technology,* September 2010, Vol. 38, No. 3, pp. 228-244. doi: 10.2346/1.3481696
13. L. Chen, M. Bian, Y. Luo and K. Li, "Maximum Tire Road Friction Estimation Based on Modified Dugoff Tire Model," *2013*

International Conference on Mechanical and Automation Engineering, Jiujang, 2013, pp. 56-61.
doi: 10.1109/MAEE.2013.24

14. P. Guarneri, G. Rocca and M. Gobbi, "A Neural-Network-Based Model for the Dynamic Simulation of the Tire/Suspension System While Traversing Road Irregularities," *IEEE Transactions on Neural Networks*, vol. 19, no. 9, pp. 1549-1563, Sept. 2008. doi: 10.1109/TNN.2008.2000806
15. M. Acosta, S. Kanarachos and M. E. Fitzpatrick, "Optimized tire force estimation using extended Kalman filter and fruit fly optimization," *IECON 2017 - 43rd Annual Conference of the IEEE Industrial Electronics Society*, Beijing, 2017, pp. 4074-4079. doi: 10.1109/IECON.2017.8216698
16. Yang, X., Olatunbosun, O., and Bolarinwa, E., "Materials Testing for Finite Element Tire Model," *SAE Int. J. Mater. Manuf.* 3(1):211-220, 2010, https://doi.org/10.4271/2010-01-0418.
17. McBride, S., Sandu, C., Alatorre, A., and Victorino, A., "Estimation of Vehicle Tire-Road Contact Forces: A Comparison between Artificial Neural Network and Observed Theory Approaches," *SAE Technical Paper* 2018-01-0562, 2018,https://doi.org/10.4271/2018-01-0562.
18. Radhakrishnan, A., Rampal, H., and Ramarathnam, K., "Reduced Order Model for Tire Dynamics," *SAE Technical Paper* 2017-26-0342, 2017, https://doi.org/10.4271/2017-26-0342.
19. Pacejka HB. "Tyre and Vehicle Dynamics. 3nd edition," Oxford: Butterworth–Heinemann, 2012.
20.
21.
22. Canudas de Wit, C., Olsson, H., Astrom, K.J., and Lischinsky, P., "A New Model for Control of Systems with Friction," *IEEE Transactions on Automatic Control*, Vol. 40, No. 3, pp. 419-425, 1995.
23. Canudas de Wit, C., Tsiotras, P., "Dynamic Tire Friction Models for Vehicle Traction Control," *Proceedings of the 38th Conference on Decision & Control*, Phoenix, AZ, pp. 3746-3751, 1999.
24. Canudas de Wit, C., Horowitz, R. and Tsiotras, P., "Model-Based Observers for Tire/Road Contact Friction Prediction," In *New Directions in Nonlinear Observer Design*, Nijmeijer, H. and T.I Fossen (Eds), Springer Verlag, Lectures Notes in Control and Information Science, May 1999.
25. Castellvi, M.C., "Benchmark of Tyre Models for Mechatronic Application," Cranfield University, 2011.
26. Buggaveeti, S., Batra, M., McPhee, J., and Azad, N., "Longitudinal Vehicle Dynamics Modeling and Parameter Estimation for Plug-in Hybrid Electric Vehicle," *SAE World Congress*, 2017.
27. Batra, M., McPhee, J., and Azad, N., "Parameter Identification for a Longitudinal Dynamics Model based on Road Tests of an Electric Vehicle," *ASME IDETC2016-59732*, 2016.
28. Olofsson, B., Lundahl, K., Berntorp, K., Nielsen, L., "An Investigation of Optimal Vehicle Maneuvers for Different Road Conditions." *IFAC Proceedings Volumes*, Vol 46, Issue 21, pg 66-71, 2013.
29. MSC Software, "Using Adams/Tire," Adams (MD R3) – Adams Docs, December 2009
30. Pearson, M., Blanco-Hague, O., and Pawlowski, R., "TameTire: Introduction to the Model. Tire Science and Technology" April-June 2016, Vol. 44, No. 2, pp. 102-119.
31. Schmeitz, A., Versteden, W., Eguchi, T., Road Load Simulation using the MF-Swift Tire and OpenCRG Road Model, SAE Technical Paper 2011-01-0190, 2011.
32. I.J.M. Besselink, A.J.C. Schmeitz, and H.B. Pacejka, An Improved Magic Formula/Swift Tyre Model That Can Handle Inflation Pressure Changes. Vehicle System Dynamics [0042-3114] Besselink, 2010, Vol. 48, Iss. S1, pp. 337
33. Pottinger, M., Pelz, W., and Falciola, G., "Effectiveness of the Slip Circle, "COMBINATOR", Model for Combined Tire Cornering and Braking Forces When Applied to a Range of Tires," SAE Technical Paper 982747, 1998
34. Brach, R., Brach, M., "The Tire-Force Ellipse (Friction Ellipse) and Tire Characteristics" *SAE International*, 2011-01-0094. 2011
35. ISO 4138:2012(en) Passenger cars — Steady-state circular driving behaviour — Open-loop test methods
36. ISO 3888-1:1999(en) Passenger cars — Test track for a severe lane-change manoeuvre — Part 1: Double lane-change
37. ISO 3888-2:2011(en) Passenger cars — Test track for a severe lane-change manoeuvre — Part 2: Obstacle avoidance
38. ISO 7401:2012(en) Road vehicles — Lateral transient response test methods — Open-loop test methods
39. A&D Technology. https://www.aanddtech.com/
40. P. Fevrier, G. Fandard, "A new Thermal and Mechanical Tire Model for Handling Simulation," January 2007
41. B. Durand-Gasselin, T. Dailliez, M. Mössner-Beigel, S. Knorr, J. Rauh, "Assessing the thermo-mechanical TaMeTirE model in offline vehicle simulation and driving simulator tests," *Vehicle System Dynamics*, Vol 48, pp

211-229, December 2010
42. M. Naoshi, K. Kazuyuki, "A Study of the Cornering Force by use of the Analytical Tyre Model," *Vehicle System Dynamics*, Vol 43, pp. 123-134, January 2005
43. R. Rajamani, "Vehicle Dynamics and Control," Springer, 2006Vehicle Dynamics Standards Committee, "Vehicle Dynamics Terminology", SAE International, Standard J670_200801, January 2008
44. Maplesoft. https://www.maplesoft.com/
45. I. Kageyama, S. Kuwahara, "A study on tire modeling for camber thrust and camber torque," *JSAE Review, 23*(3), 325-331, 2002
46. S. Li, "Camber effect study on combined tire forces," Department of Aeronautical and Vehicle Engineering KTH Royal Institute of Technology, 2013

Acknowledgments

The authors would like to thank Maplesoft, the Natural Sciences and Engineering Research Council of Canada, the Canada Research Chairs Program, and the Ontario Centres of Excellence for funding this research.

Definitions/Abbreviations

VMS	Vehicle Measurement System
WFS	Wheel Force Sensor
WPS	Wheel Position Sensor
LGS/LDV	Laser Ground Sensor/Laser Doppler Sensor
IMU	Inertia Measurement Unit
GPS	Global Positioning System
CAN	Controller Area Network

Appendix

Pure Longitudinal Slip Pacejka Model Parameters:

B = 7.553 C = 1.754 D = 0.862 E = 0.721

Pure Lateral Slip Pacejka Model Parameters:

B = 9.488 C = 1.865 D = 1.02 E = 1.181

Combined Slip Longitudinal Pacejka Model Parameters

Sideslip: 0	B = 7.553	C = 1.754	D = 0.862	E = 0.721
Sideslip: 2	B = 7.551	C = 1.75	D = 0.831	E = 0.68
Sideslip: 5	B = 6.012	C = 1.613	D = 0.672	E = 0.638
Sideslip: 10	B = 5.42	C = 1.827	D = 0.56	E = 0.711
Sideslip: 15	B = 2.98	C = 1.711	D = 0.512	E = 0.719
Sideslip: 20	B = 2.48	C = 1.648	D = 0.47	E = 0.72
Sideslip: 25	B = 2.473	C = 1.642	D = 0.454	E = 0.72

Combined Slip Lateral Pacejka Model Parameters

Slip: 0	B = 9.488	C = 1.865	D = 1.02	E = 1.181
Slip: 0.1	B = 9.02	C = 1.67	D = 0.98	E = 0.952
Slip: 0.2	B = 8.764	C = 1.521	D = 0.93	E = 0.912
Slip: 0.3	B = 6.128	C = 1.381	D = 0.854	E = 0.256
Slip: 0.4	B = 5.213	C = 1.32	D = 0.836	E = 0.124

相似法（复合滑移部分）

夏丹华译
（吉林大学汽车仿真与控制国家重点实验室，长春·130025）
《 Tire and Vehicle Dynamics》 第三版第四章
原文作者：Hans B. Pacejka[1]
丛集作者：Igo Besselink[2]
(1. 荷兰代尔夫特理工大学 2. 埃因霍温理工大学（原 TNO 汽车）

4. 2 相似法

4. 2. 2 复合滑移工况

现在，我们将解决如何描述复合滑移工况的问题。对刷子模型的分析已经深入了解力学的产生机理，我们将使用理论滑动量σx, y（公式 3. 34 或 3. 32）和量值σ （公式 3. 40）。我们将采用相似的概念，根据公式（3. 49）评估产生侧向力和纵向力的组成，并将考虑公式（3. 50）中的轮胎拖距 t 以及包括 Fx 对公式（3. 51）中回正力矩的明确贡献。因此，我们可得到包括因外倾角产生α偏移在内的理论滑动量：

$$\sigma_x = \frac{\kappa}{1+\kappa} \tag{4. 27a}$$

$$\sigma_y^* = \frac{\tan\alpha^*}{1+\kappa} \tag{4. 27b}$$

$$\sigma^* = \sqrt{\sigma_x^2 + \sigma_y^{*2}} \tag{4. 28}$$

$$\alpha^* = \alpha + \frac{C_{F\gamma}(F_z)}{C_{F\alpha}(F_z)}\gamma \tag{4. 29}$$

在随后的理论中，我们将利用理论滑移量σx 和σ*y（4. 27a, b）。通过这些量，可得到 Fy 关于 Fx 曲线图在 Fx=0 处的常数项α斜率，如图 3. 13 中的刷子模型。然而应注意的是，经验表明使用实际滑移量σx 和σy（即：κ和α*，可通过省略（4. 27a，b）中的分母再次获得）可能会得到非常好的结果，如图 4. 8 中所示。注意，当接近车轮锁定时σx→∞，此时需要人为地在(4. 27a)分母上加上一个小的正数来加以限制。

由于我们处理的是一般的非各向同性轮胎，所以会得到纯纵向和纯侧向滑移特性，这两者的特性是不相同的(参加图 4. 5)。

尽管如此，我们仍将 take 研究横向和纵向分量，但随后将分别分析 Fyo 和 Fxo 纯滑动特性。如果要用理论滑移量σ，就必须要有以σx 和σy 为横坐标的纯滑移特性。

这可以通过使用公式（4. 27a）计算每个κ值的σx 值后对原始数据进行拟合来实现，同样，将α转换为 tanα并表示结果函数：Fxo(σx)，Fyo(σy)和 MZo(σy)。或者更简单，通过替换现有纯滑移的力和力矩函数，由实际滑移量表示，参数α(弧度制)由 tanα(可以接受的

近似)表示，κ 由下面的表达式表示（源自公式（4. 27a））。

$$\kappa = \frac{\sigma_x}{1-\sigma_x} \tag{4. 30}$$

如果 Fx 特性适用于 κ 的正（行驶）和负（制动）值整个范围，这将是成功的。

否则，如果只有制动一侧可用（κ 和 σ x<0），并且驱动一侧采用制动一侧的建模来镜像，则最好采用：

$$\kappa = \frac{\sigma_x}{1+|\sigma_x|} \tag{4. 30a}$$

如果将得到的 F_x 与 σ_x 函数作图，则该曲线是对称的。然而，如果使用公式（4. 30）将横坐标转换为 κ，则产生的 $F_x(\kappa)$ 曲线会变得不对称，制动一侧与开始时的特征相同。第 3 章所讨论的刷子模型已经发现这种不对称。在我们采用的复合滑移模型中，纵向和横向力分量是根据调整后的公式（3. 49）得出，其中侧向力 $F(\sigma)$ 被 $F_{yo}(\sigma)$ 替换，而对于纵向力 $F(\sigma)$ 被 $F_{xo}(\sigma)$ 替换。图 4. 6 说明了该过程。该图显示了力矢量是如何由单个纯滑动特性产生的。在小滑移条件下，由于滑动刚度的差异，力矢量与滑动速度矢量 V_s 的方向不相反。然而，在车轮抱死时，力矢量与打滑速度矢量相反，因为这里假定，对于接近无穷大的打滑时，个体特征（渐近线）的水平是相同的（在魔术公式中，$\mu_{yo}\sin(1/2\pi C_y) = \mu_{xo}\sin(1/2\pi C_x)$）。

接下来，我们应该认识到，通过公式（4. 18）外倾角已经被考虑，因此，σ_y 将被由公式（4. 27b）定义的 σ^*_y 所取代。由此产生的力和力矩函数用 $F_{xo}(\sigma)$、$F_{xo}(\sigma)$ 与 $M_{zo}(\sigma^*_y)$ 表征。因此，可用 σ^* 表示理论滑动矢量（公式 4. 28）的大小。

$$F_x = \frac{\sigma_x}{\sigma^*} F_{xo}(\sigma^*), F_y = \frac{\sigma_y^*}{\sigma^*} F_{yo}(\sigma^*) \tag{4. 31}$$

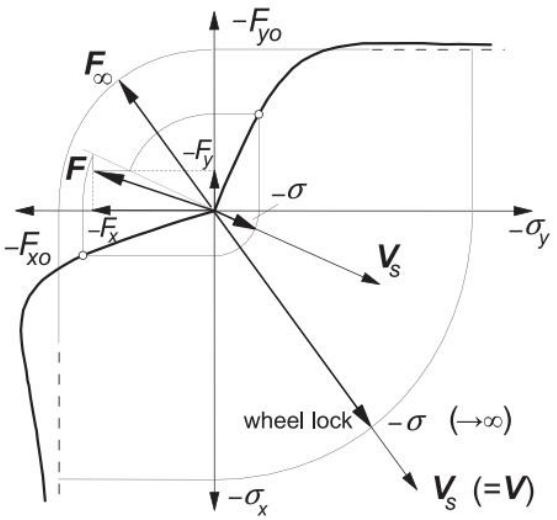

图 4. 6 根据公式（4. 31）（不考虑外倾角）由纯滑移特性得到复合滑移力

在大滑移情况下，模型显然不能正确地解释外倾角的贡献。在车轮抱死时，期望侧向力在

侧偏角零点位置也为零。模型中的情况并非如此，这是因为公式（4. 27b）且由公式（4. 18）给定 α^*时对等效理论侧滑的定义。

对于回正力矩，我们可以定义：

$$M_z = M_z^{'} + M_{zr} - c_9 a_0 \frac{F_x F_y}{F_{zo}} - c_{10} a_0 F_x - c_{11} b\gamma F_x \tag{4. 32}$$

第一项直接归因于侧向力。这个术语可以写成：

$$M_z^{'} = -t(\sigma^*) \cdot F_y \tag{4. 33}$$

结合公式（4. 31），则变为：

$$M_z^{'} = \frac{\sigma_y^*}{\sigma^*} M_{zo}^{'}(\sigma^*) \tag{4. 34}$$

公式（4. 32）的最后三项是由纵向力施加的力矩引起的，因为回正力臂是通过侧向力引起的偏转、作用线可能的初始偏移以及由于外倾角导致的轮胎横截面侧向滚动产生的。为了简单起见，假设这些影响不受车轮载荷的影响。

利用纯滑移力 Fx, yo 和力矩 M’ zo 的相似表达式，得到了复合滑移条件下的公式。对于纵向力：

$$F_x = \frac{\sigma_x}{\sigma^*} \frac{\mu_x F_z}{\mu_{xo} F_{zo}} F_{xo}(\sigma_{eq}^x) \tag{4. 35}$$

纵向方向的等效滑移为：

$$\sigma_{eq}^x = \frac{C_{F\kappa o}(F_z)}{C_{F\kappa o}} \frac{\mu_{xo} F_{zo}}{\mu_x F_z} \sigma^* \tag{4. 36}$$

对于侧向力：

$$F_y = \frac{\sigma_y^*}{\sigma^*} \frac{\mu_y F_z}{\mu_{yo} F_{zo}} F_{yo}(\sigma_{eq}^y) \tag{4. 37}$$

侧向的等效滑移为：

$$\sigma_{eq}^y = \frac{C_{F\alpha}(F_z)}{C_{F\alpha o}} \frac{\mu_{yo} F_{zo}}{\mu_y F_z} \sigma^* \tag{4. 38}$$

对于回正力矩：

$$M_z = \frac{\sigma_y^*}{\sigma^*} \frac{\mu_y F_z}{\mu_{yo} F_{zo}} \frac{C_{M\alpha}(F_z)}{C_{M\alpha o}} \frac{C_{F\alpha o}}{C_{F\alpha}(F_z)} M_{zo}^{'}(\sigma_{eq}^y) + M_{zr} - c_9 a_0 \frac{F_x F_y}{F_{zo}} - c_{10} a_0 F_x - c_{11} b\gamma F_x \tag{4. 39}$$

对于残留回正力矩：

$$M_{zr} = \frac{C_{M\gamma}(F_z) + t(F_z)C_{F\gamma}(F_z)}{1 + c_7(\sigma_{eq}^{y})^2}\gamma \qquad (4.40)$$

有个算例，表 4.1 中列出了三个附加的无量纲参数 C9、C10 和 C11。

对于与参考值不同的载荷和存在外倾角的情况，使用上述方程评估了轮胎侧向力和回正力矩的复合滑移特性。图 4.7a 和 b 给出了以侧偏角 α 为参数的结果图。由于在推导过程中使用了理论滑移量（4.27a 与 4.27b），我们发现 Fy 与 Fx 曲线在 Fx=0 附近有轻微的斜率，这也在物理刷子模型中被观察到，有时在实验评估特性中更为明显（图 3.18）。当引入外倾角（参见图 3.35c，顶部）时，不会出现导致扭转柔度的附加斜率。需要一种特别的表达式来表示这种效果。在下一节中，我们将讨论与魔术公式轮胎模型相关的问题。

可以进一步指出，由公式（4.35-4.40）、（4.27a，b）、（4.28）及参考的纯滑移函数给出的相似法模型，在下列极端情况下确实很好地表征了实际的轮胎稳态行为：（1）在纯滑移情况下；（2）在线性化复合滑移情况（小的侧偏角 α 和滑移率 κ）；（3）在车轮抱死的情况下（γ=0）。如图 4.6 所示，模型正确地表明，当车轮抱死时，所产生的力作用于与滑动速度矢量 Vs 相反的方向，如果在原始参考纯滑移曲线中，当两个滑移分量接近无穷大时（由魔术公式中的参数 μ 和 C 控制），Fxo 和 Fyo 的水平趋于同一水平。其他的滑移组合可能会引起与测量特性相关的偏差。值得注意的是，当忽略回正力矩参数 C9、C10 和 C11 时，复合滑动性能可以被表征而无需依赖复合滑动测量数据。

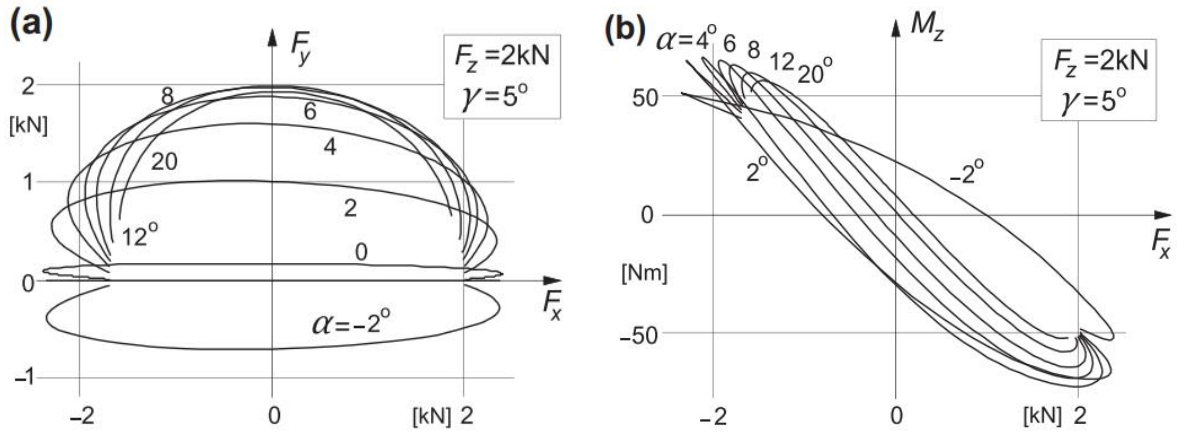

图 4.7（a）用相似法计算新荷载和外倾角条件下的侧向力 vs 纵向力；
（b）用相似法计算新载荷和外倾角条件下的回正力矩 vs 纵向力。

图 4.8 给出了与测量数据的比较。这里使用相似法，在推导阶段（在 eqns（4.35－4.38））也使用实际滑动变量 k 和 tan a（即：sx 和 sy）代替理论滑动量。在复合滑移情况下，这种客车轮胎得到了较好的一致性。

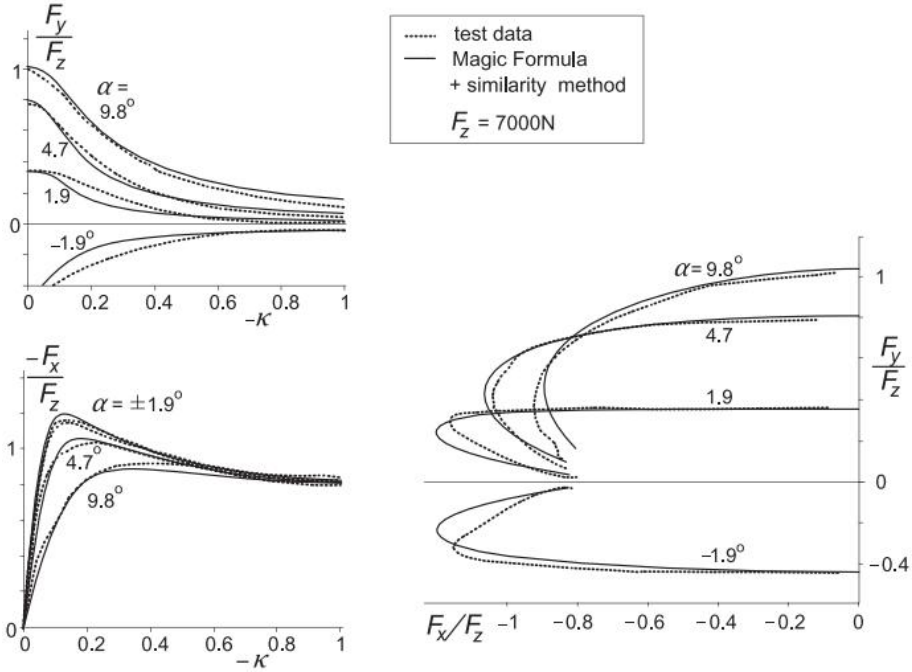

图 4. 8 用 Delft 轮胎试验挂车测量得到的轮胎复合滑移特性与用相似法计算的曲线比较

4. 2. 3 F_x 作为输入变量的复合滑移工况

在不包括车轮转动自由度的简单车辆动力学仿真研究中，更倾向于使用纵向力 F_x 作为输入量而非纵向滑移κ。这种方法几乎完全用于早期车辆动力学研究。然而，对于（准）稳态转弯分析，特别是在赛车界的电路模拟，这种选择仍然很流行。使用该方法的一个重要限制是，假设在车轮抱死时，F_x vs κ特性（尽管未使用）在整个纵向滑动范围内均为正斜率 F_x=-μF_z，或者我们仅使用位于在两个峰值之间的部分特性。这就意味着，F_y 与 F_x 曲线在 F_x 范围内是单值的。此外，假设纵向和横向的摩擦系数相同，并用μ表示。

引入纵向力 F_x 对侧向力的显著影响是降低可产生的最大侧向力。为了实现这一点，将公式（4.23）和（4.25）的右侧表达式乘以系数。

$$\varphi_x = \frac{\sqrt{\mu^2 F_z^2 - F_x^2}}{\mu F_z} \tag{4.41}$$

而表达式（4.24）要除以相同的因子。通过该操作，侧偏刚度和回正刚度不会受到影响。然而，这些刚度取决于纵向力，因为从图 3.13 的曲线可以明显看出，这属于小侧滑角。以下函数可作为实际关系的粗略近似值：

$$C_{F\alpha}(\mu, F_z, F_x) = \varphi_{x\alpha}\{C_{F\alpha}(F_z) - \frac{1}{2}\mu F_z\} + \frac{1}{2}(\mu F_z - F_x) \tag{4.42}$$

$$\varphi_{x\alpha} = \{1 - (\frac{F_x}{\mu F_z})^n\}^{1/n} \tag{4.42a}$$

根据用户的意愿，可以选择 2-8 范围内的 n 值（或多或少的曲线特征 $C_{F\alpha}(F_x)$））。对于 h 回正刚度，我们可以使用以下公式：

$$C_{M\alpha}(\mu,F_z,F_x)=\varphi_x{}^2C_{M\alpha}(F_z) \tag{4.43}$$

与外倾刚度相似：

$$C_{F\gamma}(\mu,F_z,F_x)=\varphi_x{}^2C_{F\gamma}(F_z) \tag{4.44}$$

外倾力矩刚度可以忽略不计。自由滚动轮胎的载荷相关性 $C_{F,M\alpha}(F_z)$、$C_{F\gamma}(F_z)$已经公式（4.24,4.25）中表征。可以确定，当 $F_x\rightarrow\mu F_z$（车轮驱动旋转，$\kappa\rightarrow\infty$）时，本模型确保侧偏刚度消失；而在 $F_x=-\mu F_z$（车轮抱死，$\kappa=-1$）时，侧滑刚度等于μF_z，这是正确的。F_x 函数关系式（4.21，4.22）不再起作用，摩擦系数μ_y已被μ代替。所施加的纵向力应保持在边界$-\mu F_z\cos\alpha \leqslant F_x\leqslant\mu F_z$ 内。

侧向力、回正力矩与纵向力的关系表达式（纵向力作为输入量之一），可通过以下来表示。

对于侧向力：

$$F_y=\varphi_x\frac{\mu F_z}{\mu_o F_{zo}}F_{yo}(\alpha_{eq}) \tag{4.45}$$

等效侧偏角为：

$$\alpha_{eq}=\frac{1}{\varphi_x}\frac{C_{F\alpha}(\mu,F_z,F_x)}{C_{F\alpha o}}\frac{\mu_o F_{zo}}{\mu F_z}\frac{\mu_o F_{zo}}{\mu F_z}(\alpha+\frac{C_{F\gamma}(\mu,F_z,F_x)}{C_{F\alpha}(\mu,F_z,F_x)}\gamma) \tag{4.46}$$

对于回正力矩：

$$M_z=\varphi_x\frac{\mu F_z}{\mu_o F_{zo}}\frac{C_{M\alpha}(\mu,F_z,F_x)}{C_{M\alpha o}}\frac{C_{F\alpha o}}{C_{F\alpha}(\mu,F_z,F_x)}M_{zo}(\alpha_{eq})+M_{zr}-c_9a_0\frac{F_xF_y}{F_{zo}}-c_{10}a_0F_x-c_{11}b\gamma F_x \tag{4.47}$$

最后一项取自公式（4.39），残留回正力矩为：

$$M_{zr}=\varphi_x\frac{C_{M\gamma}(F_z)+t(F_z)C_{F\gamma}(F_z)}{1+c_7\alpha^2}\gamma \tag{4.48}$$

第 4.3 节末尾的练习题 4.1 中讨论了使用相似法技术评估侧向力特性的问题，其中纵向力被视为输入量之一。

在第 4.3 节中，将详细介绍魔术公式轮胎模型。这个复杂的模型更加精确，将再次使用纵向滑移κ作为输入变量。

行业先锋

浦林成山（山东）轮胎有限公司研发实力简介

浦林成山（山东）轮胎有限公司创立于 1976 年，是一家专注于轮胎研发、制造和销售的现代化企业，是中国最具影响力的轮胎企业之一。浦林成山产品包括乘用车轮胎、商用车轮胎、工业轮胎、农业轮胎及特种车辆轮胎五大系列，旗下拥有四大品牌，包括中高端品牌“浦林（Prinx）”及驰名品牌“成山（Chengshan）”、“澳通(Austone)”与“富神（Fortune）”。“成山”牌轮胎被认定为“中国名牌”、“中国驰名商标”、“中国轮胎市场产品质量用户满意品质信誉第一品牌”，成为轮胎行业唯一的“三冠王”。公司在全球各地拥有超过 470 多家合作经销商，遍布世界 130 多个国家及地区。

公司研发实力雄厚，拥有国家级企业技术中心、博士后工作站，设有青岛工业研究设计中心、荣成轮胎测试中心。公司围绕轮胎全生命周期制造的纳米级原材料、创新型制造工艺、数字化、网络化、信息化、智能化、仿真分析等各个环节开展工作，逐步形成四大创新平台。山东省制造业创新中心首批创新中心；首次提出了多尺度轮胎全生命周期概念，“轮胎多尺度全生命周期制造创新中心”是山东省轮胎行业唯一一家创新中心；加大对新能源汽车轮胎的研究力度，联合国内外高校和企业 12 家成立“新能源汽车轮胎协同研究室”。

图 1　四大创新平台

数字化轮胎技术研发平台-采用轮胎功能-技术分解矩阵工具，将部件功能进行转化或引入新的物质，优化轮胎内部结构设计，调整轮胎受力至最佳状态，充分发挥轮胎节能、环保和安全的特点。轮胎自动三维建模技术，实现轮胎三维模型的参数自动化，提高新产品开发效率及准确率。围绕产品轻量化、低滚阻、耐磨性三大重点，推行“三低三高”的生产工序研究，三低即低温炼胶、低收缩挤出、低排放硫化；三高即高分散、高密度、高性能。

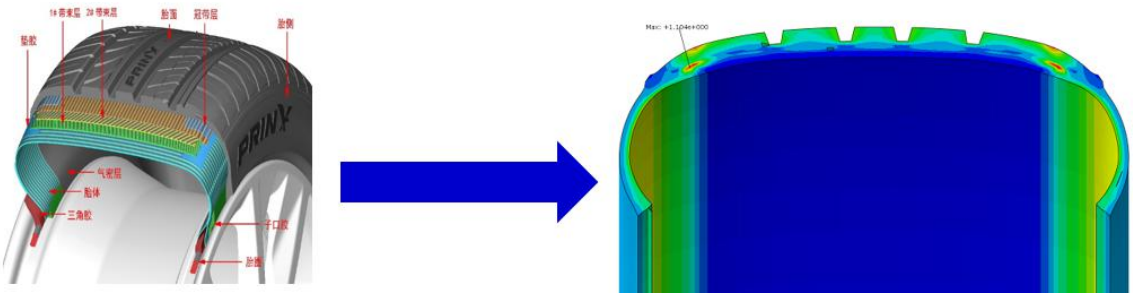

图 2　数字化轮胎技术研发平台

轮胎仿真与设计系统-Prinx-TDSS 在 NX、HYPERMESH、ABAQUS 基础上进行自主二次开发，拥有完全软件知识产权。

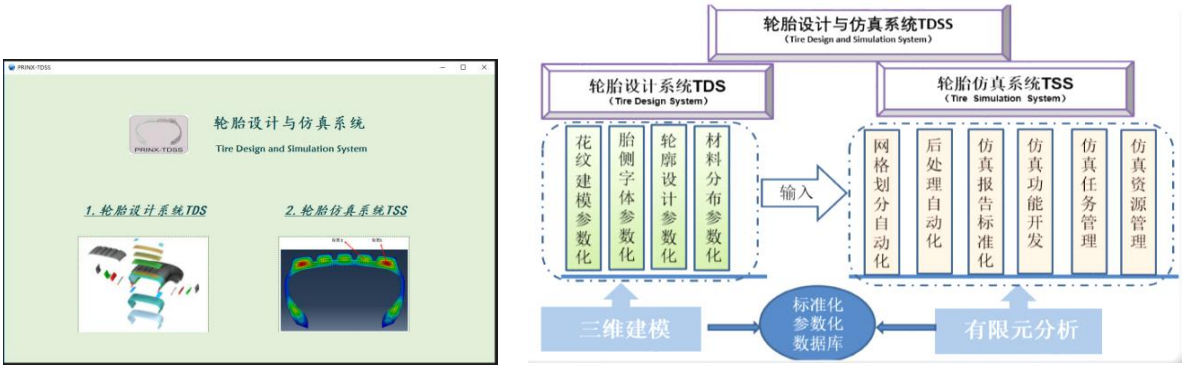

图 3　轮胎设计与仿真系统

轮胎设计系统-基于 NX 自主二次开发，实现花纹设计和扩展参数化，提高效率；软件后台集成轮廓设计理论和设计规范，保证设计产品性能一致性。

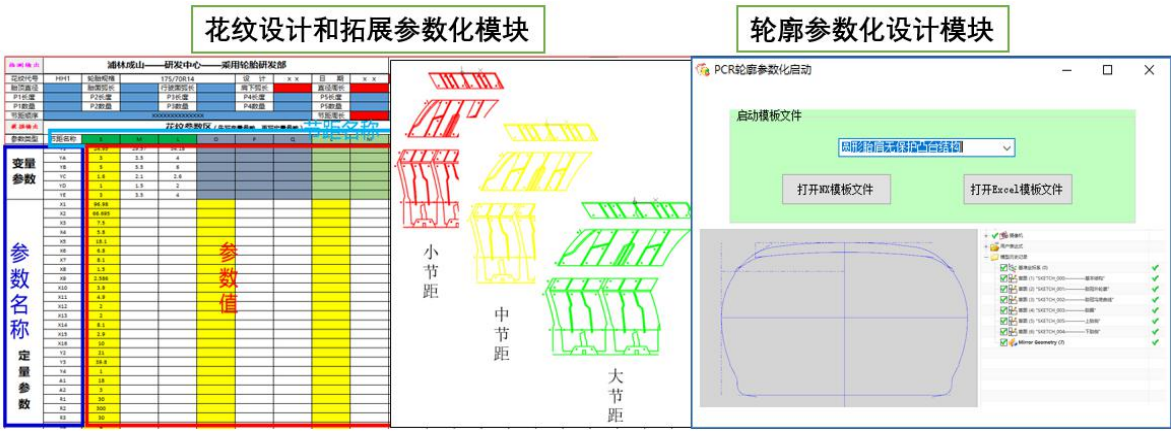

图 4　轮胎设计系统

轮胎仿真系统-基于 ABAQUS、hypermesh 等软件并进行二次开发，可实现轮胎尺寸、印痕刚度、滚动阻力、温度场、模态、花纹节距优化、轮胎六分力、轮胎耐久、轮胎磨耗、整车操控性能等仿真，通过仿真全面评估产品性能。

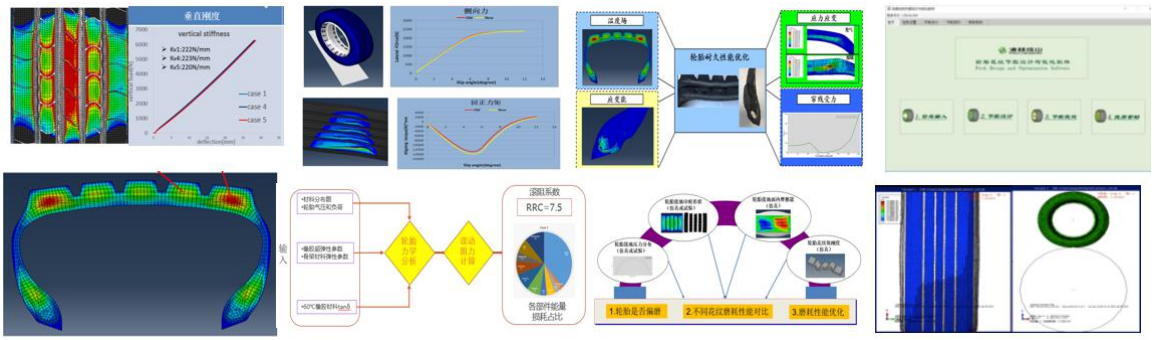

图 5　轮胎仿真系统

在轮胎动力学领域，公司开展了轮胎操稳客观评价体系的研究，根据整车悬架 K&C、转向系统、减震系统、轮胎六分力试验数据等测试结果在 Carsim 中建立整车模型并仿真，进行整车操控主观和客观评价，建立了仿真与实车评价的一致性。

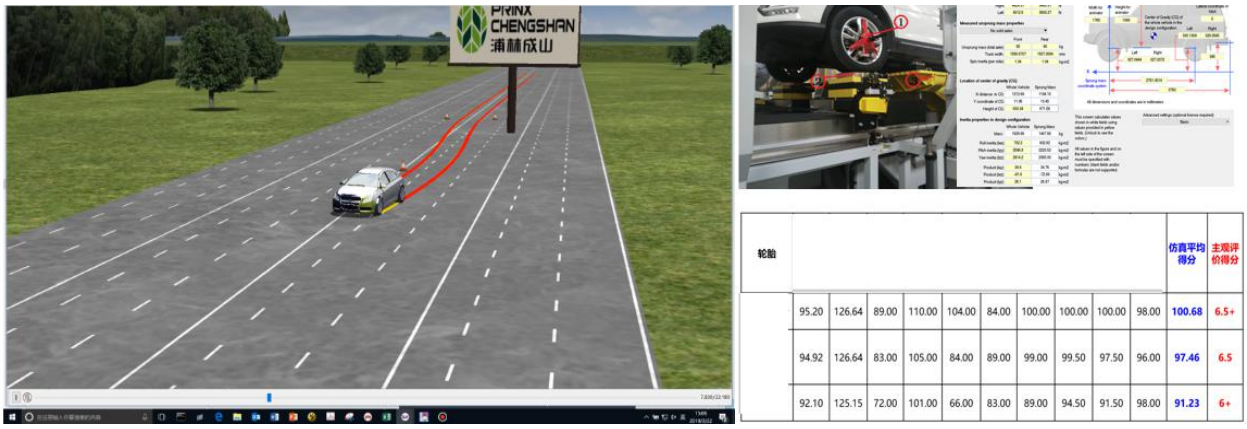

轮胎											仿真平均得分	主观评价得分
	95.20	126.64	89.00	110.00	104.00	84.00	100.00	100.00	100.00	98.00	100.68	6.5+
	94.92	126.64	83.00	105.00	84.00	89.00	99.00	99.50	97.50	96.00	97.46	6.5
	92.10	125.15	72.00	101.00	66.00	83.00	89.00	94.50	91.50	98.00	91.23	6+

图 6　在 Carsim 中建立整车模型并仿真，进行整车操控主观和客观评价

在研发设备方面，荣成测试中心投资 2.3 亿，建设 46 个研发试验室，购置仪器设备 177 台（套），是集轮胎原材料应用研究、物理/化学分析测试、成品轮胎性能评价、车辆与轮胎性能匹配为一体的行业领先研发平台。

图 7 荣成测试中心部分设备

浦林成山轮胎作为轮学盟的副理事长单位，将继续积极参与联盟各项工作和科研项目，与联盟成员同心协力，为中国轮胎动力学发展做出应有的贡献。

苏州同元系统建模仿真软件及其在轮胎动力学仿真中的应用

同元软控 TONG YUAN

一、苏州同元简介

苏州同元软控信息技术有限公司成立于 2008 年，是为装备制造业系统设计提供工业软件产品研发、工程服务及系统工程整体解决方案的高新技术企业。同元软控的产品和服务已经广泛应用于航天、航空、能源、车辆、船舶、教育等行业，为大飞机、航空发动机、空间站、嫦娥工程、大推力运载火箭等国家系列重大工程提供数字化设计支撑。

同元软控经过 18 年技术积累、10 年持续研发，全面掌握自 CAD、CAE 之后的新一代数字化核心技术——系统多领域统一建模与仿真技术，形成目前核心产品——系统设计与仿真验证平台 MWorks。

二、同元产品介绍

MWorks 是同元软控基于国际知识统一表达与互联标准打造的系统设计与仿真验证平台，MWorks 采用基于模型的方法全面支撑系统设计，通过不同层次、不同类型的仿真来验证系统设计，形成<设计-验证>对偶，构建系统数字化设计与验证闭环。其中 MWorks.Sysplorer 是面向多领域装备产品的系统级统一建模与仿真验证软件。

基于国际多领域统一建模规范 Modelica，MWorks.Sysplorer 支持工业设计知识的模型化表达和模块化封装，支持基于物理拓扑的快速系统模型集成与仿真验证，支持多方案优选及设计参数优化。利用现有大量可重用的 Modelica 专业库，MWorks.Sysplorer 可以广泛地满足机械、液压、控制、电子、气压、热力学、电磁等专业，以及航空、航天、车辆、船舶、能源等行业的知识积累、仿真验证与设计优化需求。

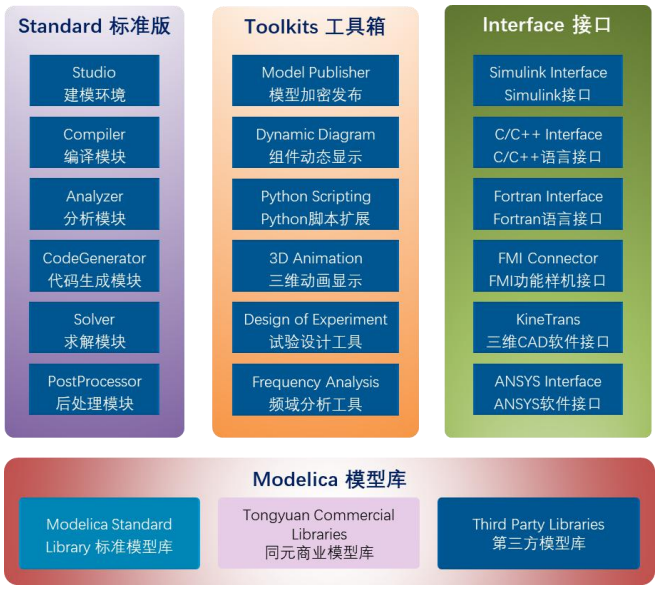

图 1 系统建模仿真软件 MWorks.Sysplorer 模块结构图

三、系统仿真飞机刹车系统与轮胎动力学应用

为了加快开发进程，缩短研发周期，并提高产品综合性能和品质，目前国外先进的航空制造商都积极地在多学科系统集成与整机数字建模仿真方面进行技术探索和应用。

结合飞机研制流程，基于 MWorks.Sysplorer 建立了飞机级虚拟综合集成试验系统，可用于飞机系统型号初期的验证、系统各系统集成接口验证、针对各类飞行工况的模拟、极限工况的功能性能分析等，从而对飞机系统设计需求进行验证与确认，并为飞机物理综合试验提供预先的技术保障。

虚拟综合集成试验系统完成了起落架、飞控、液压、环境谱等多领域模型库的开发，并实现了多领域系统虚拟试验科目分析，其中飞机刹车系统综合建模仿真分析就是重要的一环。飞机刹车系统模型包括液压子系统、控制子系统、机械子系统。

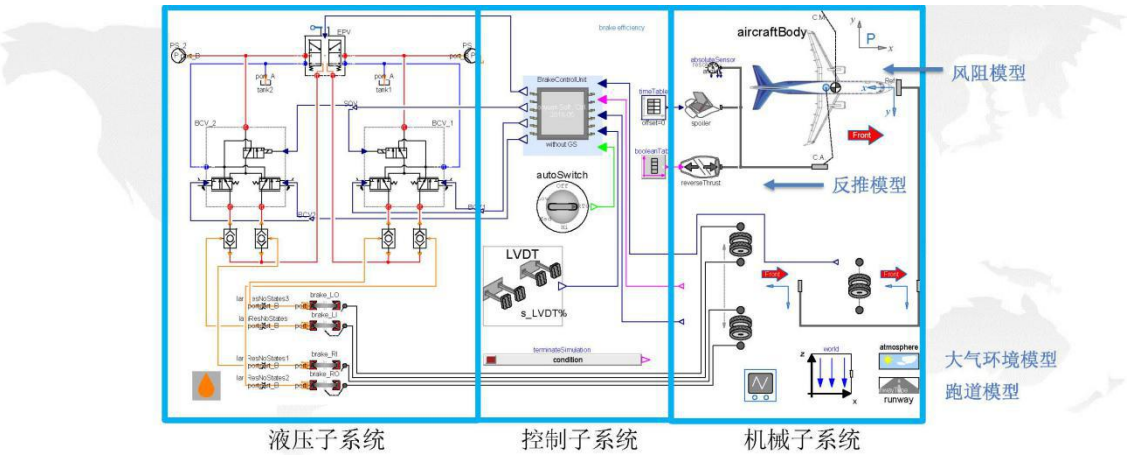

图 2 飞机刹车系统模型图

通过动力学相关公式构建轮胎模型与刹车系统机构模型：

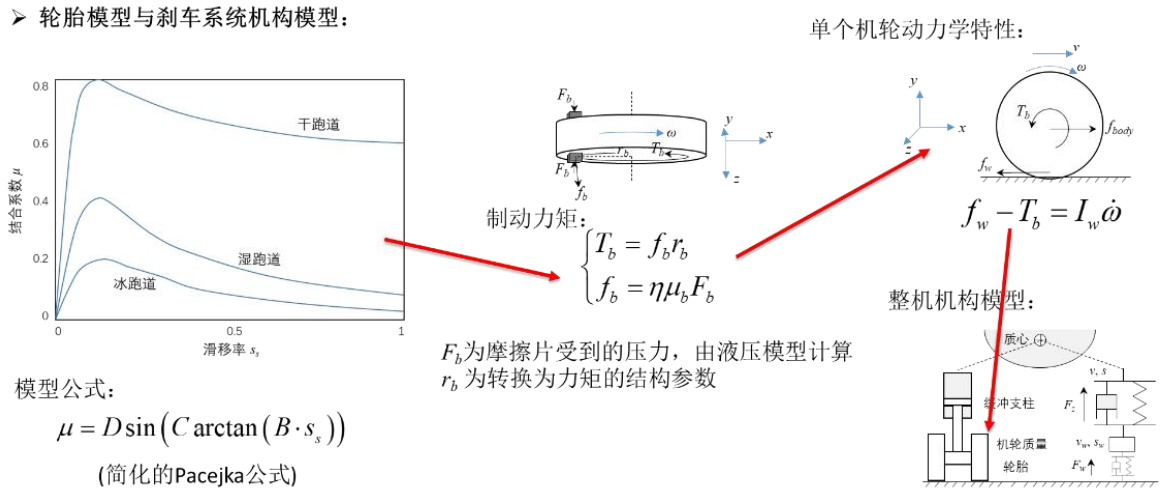

图 3 刹车系统机构与轮胎模型（1）

➢ 轮胎模型与刹车系统机构模型：

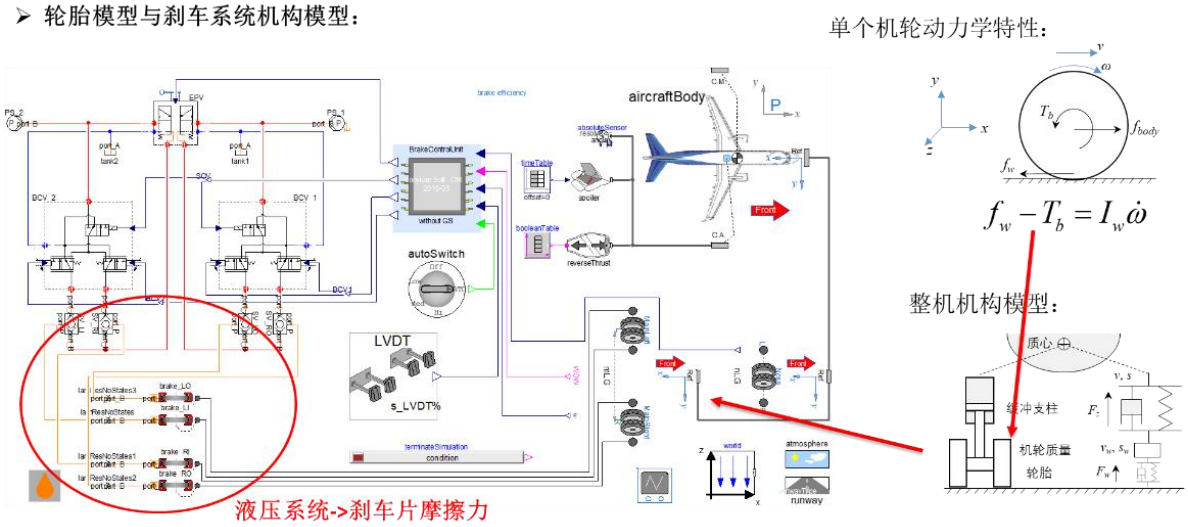

图 4 刹车系统机构与轮胎模型（2）

在 MWorks.Sysplorer 中分别进行仿真，得到湿跑道、冰跑道等路况下刹车性能分析结果：

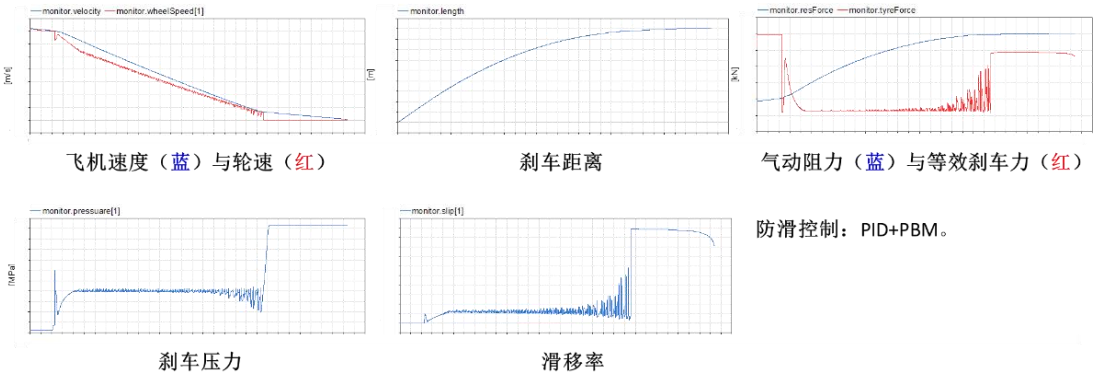

图 5 湿跑道工况下刹车性能分析结果

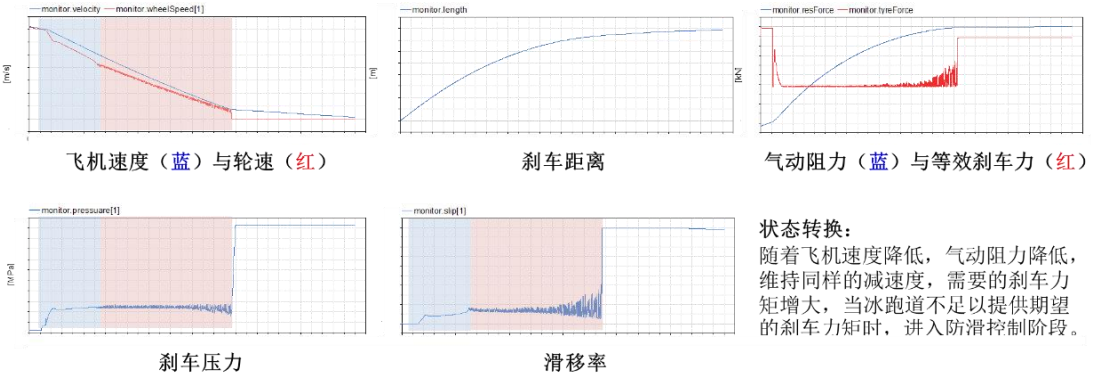

图 6 冰跑道工况下刹车性能分析结果（自动刹车）

基于MWorks.Sysplorer，可以方便地建立轮胎动力学及其所在的飞机刹车系统的模型并进行仿真分析，这种方式同样可以用于车辆系统的轮胎动力学建模仿真。MWorks.Sysplorer为轮胎动力学仿真分析提供了新一代可视化多领域统一建模仿真工具，并支持轮胎在系统环境下的整体仿真分析。同元软控期待与轮学盟各成员单位协同合作，充分发挥系统仿真在轮胎动力学方面应用的发展潜力，提供自主可控、易用可扩展的轮胎动力学建模仿真分析软件。

青岛森麒麟轮胎股份有限公司研发实力简介

一、企业简介

青岛森麒麟轮胎股份有限公司是一家专注于绿色、高品质、高性能的高端半钢子午线轮胎及航空轮胎的研发与生产的轮胎制造企业。公司首创中国轮胎工业 4.0 智慧工厂，并积极响应国家“一带一路”倡议，借助青岛工厂成功实践的智能制造经验，在泰国建成全球领先的轮胎制造生产基地，为公司“3+1”战略奠定基础。

公司拥有完善的境外轮胎替换市场销售体系，产品远销150多个国家和地区，同时也在逐步打入国内外整车企业供应商体系，稳步攻坚全球配套市场，坚持“创世界一流轮胎品牌”目标，离不开技术突破及其产业化应用、智能制造模式实践，产能科学布局。

二、研发能力

青岛森麒麟轮胎股份有限公司技术力量雄厚，拥有一支高素质、高水平，覆盖领域广，知识层次结构合理，具有活力、稳定的专业研发队伍。在半钢子午线轮胎领域，拥有逾7000个细分规格产品，具备全尺寸半钢子午线轮胎制造能力，产品广泛应用于各式轿车、越野车、城市多功能车、轻卡及皮卡等车型，在航空胎领域，成功开发适配于播音737系列等多种机型的多规格产品

公司掌握超高性能轿车子午线轮胎技术，超低滚阻、高抗湿滑的高性能子午线轮胎技术，30-32英寸超大尺寸高性能轮胎技术，F4方程式赛车胎技术，四季型缺气保用轮胎技术，石墨烯导静电轮胎技术等多项自主研发核心技术，奠定了公司在行业内的领先地位。

三、测试能力

公司检测中心集产品测试、数据分析、技术研究为一体，负责轮胎性能研究、轮胎材料分析研究、轮胎仿真分析与测试一致性研究、试验与主观测评一致性研究等，可满足轮胎日常测试，新产品研发及自主创新需求。

(1)轮胎性能研究及轮胎材料分析研究

序号	设备名称	设备图片	设备能力
1	MTS Flat-Trac CT Plus 六分力试验机		进行轮胎力和力矩测试，轮胎操稳特性研究，轮胎动力学建模：PAC2002、Ftire 及其他轮胎模型研究；
2	ZF 轮胎高速均匀性&滚阻试验机		轮胎滚动阻力测试（力矩法）；轮胎高速均匀性测试；轮胎过 cleat 试验；轮胎平点测试；轮胎低速均匀性测试；轮胎 Run out 测试。
3	TMT-2 PCR 轮胎综合试验机	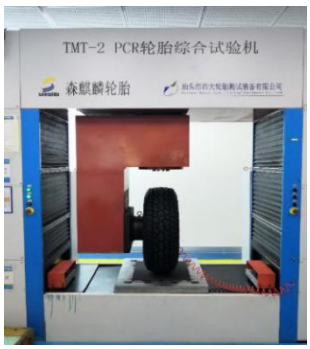	轮胎静态纵向刚度、横向刚度、径向刚度、包络刚度、扭转刚度测试；轮胎接地压力和接地印痕测试；轮胎电阻测试，最大测试量程可达 10^{12} 欧姆 。
4	轮胎 3D 轮廓扫描试验机		轮胎轮廓的逆向开发 ：高精度 2D 轮廓测量；具有冠弧半径拟合功能；轮胎磨耗分析；花纹开发和分析胎侧测量轮胎真圆度分析 轮辋测量功能
5	轮胎高温老化箱		轮胎高温老化试验，试验箱容量 40 条轮胎。

序号	设备名称	设备图片	设备能力
6	轮胎气密性试验室		共 32 个测试工位，每一检测工位均有胎压监测传感器及压力表显示，以及胎里温度检测传感器，更加符合理想气体状态方程。
7	LAT100		进行胶料的磨耗测试与变温磨耗测试、摩擦力测试、侧向力测试、滚阻性能测试；
8	RPA		进行生胶、混炼胶的温度频率、应变扫描测试；恒温、变温流变测试
9	TGA		用于测量待测样品的质量与温度变化关系，用来研究材料的热稳定性和组分。
10	DSC		测量样品由于物理和化学性质的变化而发生的焓变与温度或时间的关系。
11	水压爆破试验机		轿车&轻卡轮胎水压爆破试验和航空胎水压爆破试验 。
12	TS 航空胎动态模拟试验机		模拟航空轮胎起飞，降落，滑行，测量航空轮胎性能。

（2）轮胎仿真分析与测试一致性研究

公司拥有 Catia、UG、ABAQUS、Isight 等开发分析软件，可进行轮胎花纹、材料、结构、台架测试、实车测试等多种仿真，有效的缩短了产品开发周期、降低产品成本。提高产品质量。

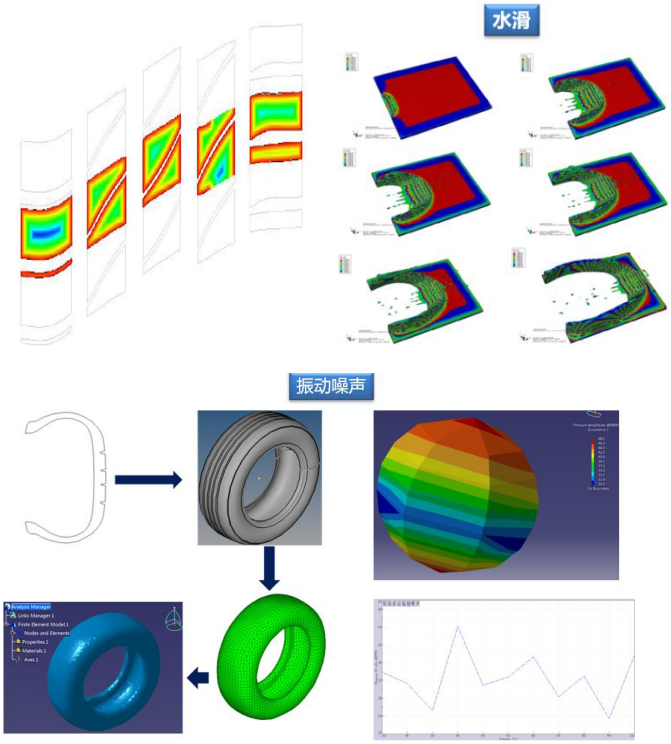

图 1 仿真分析图例

（3）试验与主观测评一致性研究

我司聘请专业车手，并与伊狄达试验场签订长期合作，测试内容涵盖轮胎干地操控性，湿地操控性，平顺性，等轮胎各项性能，保证轮胎主观测试的专业性和准确性。我司拥有强大的研究团队，通过主观测试与客观测试（台架试验）结合，构建一个更加系统科学的轮胎性能评价体系，从而提高轮胎性能，缩短开发周期，提高研发质量。

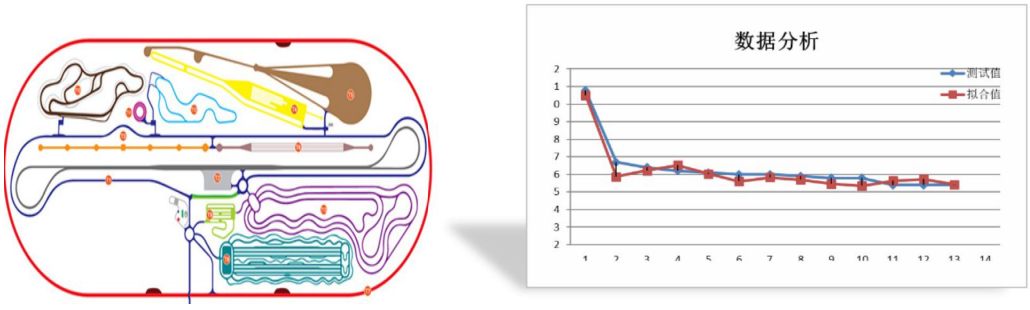

图 2 伊狄达试验场示意图及主客观测试分析结果对比

作为轮胎动力学协同创新联盟的理事单位、轮胎动力学测试联合实验室，森麒麟轮胎愿同轮学盟及各成员单位一起，为促进我国轮胎行业高质量发展不懈努力。

快讯精选

2019轮胎与车辆动力学院士论坛盛大召开

10 月 23 日，由中国汽车工程学会主办，轮胎动力学协同创新联盟承办的 2019 轮胎与车辆动力学院士论坛在上海汽车会展中心圆满落幕。本次论坛以“电动 •智能 •基础 •创新”为主题，邀请了国内外 10 位专家作技术分享，此外，论坛上设置了“高端访谈”环节，以“面向未来，我国汽车工业的挑战与机遇”为主题，邀请了整车和轮胎企业的高层领导及专家分享自己关于未来行业发展的看法。中国工程院院士、吉林大学汽车学院名誉院长、轮胎动力学协同创新联盟理事长郭孔辉先生莅临指导。

中国工程院院士、吉林大学汽车学院名誉院长、
轮胎动力学协同创新联盟理事长郭孔辉先生

上午，院士论坛在北展厅分享汇会议室举行，下午在南展厅大会议区举办。论坛共分为五个时段，第一时段由吉林大学教授、轮胎动力学协同创新联盟秘书长卢荡先生主持；第二时段由吉利汽车研究院高级技术专家唐腊梅女士主持；第三时段由东风汽车集团股份有限公司技术中心总工程师陈赣先生主持；第四时段由东风汽车集团股份有限公司技术中心副主任杨彦鼎先生主持；“高端访谈”由吉林大学教授、轮胎动力学协同创新联盟秘书长卢荡先生主持。

吉林大学教授、轮胎动力学协同创新联盟秘书长卢荡先生（左一）；
吉利汽车研究院高级技术专家唐腊梅女士（左二）；
东风汽车集团股份有限公司技术中心总工程师陈赣先生（右一）；
东风汽车集团股份有限公司技术中心副主任杨彦鼎先生（右二）

会议伊始，卢荡教授对各位领导及专家的到来表示热烈的欢迎和衷心的感谢，并宣布本次院士论坛正式开始。首先，广州汽车集团股份有限公司首席技术总监吴旭亭先生作《汽车底盘开发技术的演变与创新》演讲，从汽车底盘子系统的诞生及早期的开发技

术、车辆动力学的诞生与发展、底盘的主动控制系统等 5 个方面与大家交流分享。接下来，易航智能首席技术官金凌鸽先生发表了题为《轮胎与自动驾驶漂移》的演讲，以自动驾驶漂移为例，展示了轮胎模型对于自动驾驶车辆在极限工况下的控制影响。随后，吉林大学马尧博士以《智能车轮系统开发及其在车辆动态控制中的应用》为题分享了吉林大学智能网联车辆动力学创新团队在车辆控制中动力学关键技术、智能车轮系统开发及验证等方面的经验与技术。

广州汽车集团股份有限公司首席技术总监吴旭亭先生（左）；
易航智能首席技术官金凌鸽先生（中）；
吉林大学马尧博士（右）

一汽解放汽车有限公司商用车开发院首席工程师郭平女士发表了《商用车用户需求变化与轮胎动力学发展方向》，演讲内容包括中国商用车市场变化和用户需求变化、商用车对轮胎动力学性能的需求等四个方面。美国 Altair 中国公司技术经理马越峰先生分享了《Random analysis in full vehicle road NVH simulation》，与大家探讨了随机响应分析技术在道路 NVH 仿真中的应用。

一汽解放汽车有限公司商用车开发院首席工程师郭平女士（左）；
美国 Altair 中国公司技术经理马越峰先生（右）

下午，首先为大家带来精彩演讲的是中国工程院院士、吉林大学汽车学院名誉院长、轮胎动力学协同创新联盟理事长郭孔辉先生，郭孔辉院士以《轮胎建模中的干摩擦动力学问题》为题，详细讲解了轮胎模型的过零问题、动/静摩擦、干摩擦、滑移刚度与整车的运动阻尼等问题。随后，东风汽车集团股份有限公司技术中心副主任杨彦鼎先生以《乘用车轮胎性能开发》为题，从开发流程、关键指标对整车性能（NVH、R&H、耐久、动力经济性等）的影响等方面分享了东风在乘用车开发领域中轮胎开发的心得和体会。吉林大学教授、轮胎动力学协同创新联盟秘书长卢荡先生以《Analysis and prediction of tire cornering properties for differentinflation pressure based on deflection control》为题，为大家讲解基于轮胎压缩量控制的，不同胎压下轮胎侧偏特性影响分析及预测。

中国工程院院士、吉林大学汽车学院名誉院长、轮学盟理事长郭孔辉先生（左）；
东风汽车集团股份有限公司技术中心副主任杨彦鼎先生（中）；
吉林大学教授、轮胎动力学协同创新联盟秘书长卢荡先生（右）

最后两篇技术报告分别由德国 CDTire 公司产品经理 Axel Gallrein、德国 FTire 公司应用工程师 Joachim Stallmann 进行演讲，题目分别为《CDTire -- closing the gap to structural analysis》及《FTire--The market leading physical tire model》，为大家详细介绍了两种不同轮胎模型的特点和优势。

德国 CDTire 公司产品经理 Axel Gallrein（左）；
德国 FTire 公司应用工程师 Joachim Stallmann（右）

本次院士论坛最后一个环节为高端访谈，邀请了长春富晟汽车创新技术有限公司总经理刘蕴博先生、广州汽车集团股份有限公司首席技术总监吴旭亭先生、上汽通用五菱汽车股份有限公司总经理助理梅胜军先生、东风汽车集团股份有限公司技术中心副主任杨彦鼎先生、中策橡胶集团有限公司总工程师朱大为先生、山东玲珑轮胎股份有限公司研究总院高级总监魏胜先生，围绕“面向未来，我国汽车工业的挑战与机遇”的主题，主要讨论了以下方面的问题：从性能出发、着重于提高软实力、往智能化、互联化、自动驾驶、轻量化、新能源方面发展以更好地面对未来；以市场为导向，以用户为中心，与政府紧密合作的“广西模式”的实践经验；中国轮胎发展走了一条从引进到消化、吸收、创新的技术之路；东风汽车在面向新能源汽车时，在国家政策、国家基础设施建设、人才结构变化、产品开发方面所面临的挑战。

吉林大学教授、轮胎动力学协同创新联盟秘书长卢荡先生（左一）；
山东玲珑轮胎股份有限公司研究总院高级总监魏胜先生（左二）；
东风汽车集团股份有限公司技术中心副主任杨彦鼎先生（左三）；
广州汽车集团股份有限公司首席技术总监吴旭亭先生（中）；
中策橡胶集团有限公司总工程师朱大为先生（右一）；
上汽通用五菱汽车股份有限公司总经理助理梅胜军先生（右二）；
长春富晟汽车创新技术有限公司总经理刘蕴博先生（右三）

至此，本次轮胎与车辆动力学院士论坛圆满落幕。正如高端访谈的主题“面向未来，我国汽车工业的挑战与机遇”一样，轮学盟也在面临着行业中未来的挑战和机遇。面向未来，轮学盟将继续根植于轮胎动力学，带动行业创新发展，攻克行业技术难关，为行业同仁提供分享技术经验和成果交流的平台，为行业做出自己的贡献。

第三届理事会暨轮胎与车辆动力学技术论坛成功召开

10 月 24 日，轮胎动力学协同创新联盟第三届理事会暨轮胎与车辆动力学技术论坛在上海顺利召开。出席本次会议的重要嘉宾有：轮学盟理事长、中国工程院院士、吉林大学汽车工程学院名誉院长郭孔辉院士，轮学盟理事长、中国汽车工程学会常务副理事长及秘书长张进华先生，轮学盟副理事长、广州汽车集团股份有限公司汽车工程研究院副院长刘念斯先生，轮学盟副理事长、安徽江淮汽车集团股份有限公司乘用车研究院院长温敏先生，轮学盟副理事长、佳通轮胎（中国）研发中心总监李炜先生，轮学盟副理事长、倍耐力轮胎有限公司轿车轮胎研发总监鲁明诚先生，轮学盟理事、汕头市浩大轮胎测试装备有限公司陈迅总经理，中国第一汽车集团公司底盘所所长侯杰女士，万力轮胎股份有限公司总工程师罗吉良先生，浦林成山（青岛）工业研究设计有限公司总经理车宝臻先生，山东玲珑轮胎股份有限公司研究总院高级总监魏胜先生。

本次理事会议分为四个时段：1. 轮学盟理事长致辞、秘书处工作汇报及审议表决；2. 高端访谈：面向汽车市场的未来，轮胎行业调整的必要性；3. 企业技术报告；4. 高校技术报告。由万力轮胎股份有限公司总工程师罗吉良先生担任第一时段的主持人；轮胎动力学协同创新联盟秘书长、吉林大学教授担任高端访谈主持人；山东玲珑轮胎股份有限公司研究总院高级总监魏胜先生担任企业技术报告主持人；吉林大学马尧博士担任高校技术报告主持人。

在第一时段，轮学盟理事长、中国工程院院士、吉林大学汽车工程学院名誉院长，郭孔辉院士作理事长致辞，对各位专家的到来表示热烈欢迎，同时总结轮学盟去年工作，并殷切希望各位专家能够多提宝贵意见。

轮学盟理事长、中国工程院院士、吉林大学汽车工程学院名誉院长郭孔辉院士

轮学盟秘书长、吉林大学卢荡教授作 2019 年度工作汇报及 2020 年度工作计划，从联盟形象、内部管理、成员单位及重点工作四个方面汇报轮学盟 2019 年度所做的工作，主要汇报了轮学盟在政策和战略研究、关键共性技术研发、标准与法规、测试评价、产业推广、学术交流与国际合作及人才培养方面的工作进展。2020 年，轮学盟将进一步推进上述方面的工作，继续为成员单位乃至整个行业服务。

轮学盟秘书长、吉林大学卢荡教授

在工作汇报及计划结束后，万力轮胎股份有限公司总工程师罗吉良先生组织现场专家对轮学盟工作进行审议表决。与会专家对轮学盟工作提出宝贵意见并高度认可轮学盟工作，由此，轮学盟工作汇报通过专家审议。

万力轮胎股份有限公司总工程师罗吉良先生

与会专家举手表决通过轮学盟工作审议

本次会议高端访谈的主题是“面对汽车市场的未来，轮胎行业调整的必要性”，邀请了理事长郭孔辉院士、中国第一汽车集团公司研发总院底盘开发所所长侯杰女士、万力轮胎股份有限公司总工程师罗吉良先生、佳通轮胎（中国）研发中心总监李炜先生、安徽江淮汽车集团股份有限公司乘用车研究院院长温敏先生、倍耐力轮胎有限公司轿车轮胎研发总监鲁明诚先生、浦林成山（山东）轮胎有限公司总经理车宝臻先生作为访谈嘉宾，探讨了面向未来，非充气轮胎、智能轮胎在未来的发展趋势、整车企业和轮胎企业如何更好地合作、如何实现轮胎与整车

的同步开发、汽车市场的未来等问题。

倍耐力轮胎有限公司轿车轮胎研发总监鲁明诚先生；（左一）
安徽江淮汽车集团股份有限公司乘用车研究院院长温敏先生（左二）；
轮学盟秘书长、吉林大学教授卢荡先生；（左三）
万力轮胎股份有限公司总工程师罗吉良先生；（中）
浦林成山（山东）轮胎有限公司总经理车宝臻先生（右一）
佳通轮胎（中国）研发中心总监李炜先生；（右二）
中国第一汽车集团公司研发总院底盘开发所所长侯杰女士；（右三）

下午，企业技术报告正式开始。第一位演讲嘉宾是中国第一汽车集团公司研发总院底盘研发所主任郝文权先生，以《整车动力学性能开发与轮胎性能控制》为题，从红旗整车动力学性能开发、整车性能与轮胎特性的关系及轮胎性能控制三方面进行了汇报。第二位演讲的嘉宾是汕头市浩大轮胎测试装备有限公司总经理陈迅先生，演讲题目为《关注轮胎全生命周期技术性能的变化》，与大家分享国内外在磨损轮胎的测试和研究方面的进展情况，以及浩大在磨削实践中的一些观察。第三位演讲嘉宾是浙江吉利汽车研究院有限公司高级专家唐腊梅女士，通过作题为《Road Tire Spec Tuning for Vehicle Dynamics》的报告，分享了自己从业以来在整车性能开发及轮胎性能调校等方面的看法与体会。

山东玲珑轮胎股份有限公司研究总院高级总监魏胜先生（左一）；
中国第一汽车集团公司研发总院底盘研发所主任郝文权先生（左二）；
浙江吉利汽车研究院有限公司高级专家唐腊梅女士（右一）；
汕头市浩大轮胎测试装备有限公司总经理陈迅先生（右二）

高校技术报告中，国防科技大学高经纬教授以《基于多体动力学-离散元耦合的轮胎牵引特性数值仿真及试验验证》为题，讲解了基于车辆地面力学理论中的轮-壤相互作用机理及其开展的轮式车辆轮胎在砂壤路面下的多工况牵引特性研究。宁波大学黄海波教授以《考虑截面横向振动的高阶模态预测模型及应用》为题，汇报了一个基于三维环壳的轮胎振动解析模型，通过结合对应提出的位移函数，能够快速高效的预测胎径/侧向和横向（横截面方向）振动。最后，吉林大学高磊先生发表了题目为《非充气轮胎研究》的演讲报告，报告以米其林公司 2005 年发布的 Tweel 轮胎为基础，通过有限元的方法对其顶部承载和剪切带理论进行探索和验证，充分证实了非充气轮胎的力学性能优势。




吉林大学马尧博士（左一）；
国防科技大学高经纬教授（左二）；
吉林大学高磊先生（右一）；
宁波大学黄海波教授（右二）

至此，第三届理事会暨轮胎与车辆动力学技术论坛顺利结束。轮胎动力学协同创新联盟成立于 2017 年 10 月 23 日，至今已成立两年。两年的时间里，感谢成员单位及专家对轮学盟工作的支持，愿未来携手同行，继续为推动我国汽车及轮胎行业向前发展贡献力量。

轮学盟 2020 年会议计划

一、学术交流活动计划

1.国际轮胎动力学测试技术及标准研讨会

时间：3 月 24 日 -25 日

地点：上海

会议费：2800 元，理事长单位、副理事长单位、智资委专家 7.5 折，理事单位 8.5 折

2.航空轮胎动力学技术研讨会

时间：5 月 26 日

地点：西安

会议费：1800 元，理事长单位、副理事长单位、智资委专家 7.5 折，理事单位 8.5 折

3.国际轮胎动力学仿真技术及标准研讨会

时间：8 月 25 日-26 日

地点：北京

会议费：2800 元，理事长单位、副理事长单位、智资委专家 7.5 折，理事单位 8.5 折

4.轮学盟理事会及专家委员会会议

时间：12 月 3 日-4 日

地点：广州

注册费：1800 元，理事长单位、副理事长单位 2 位免费参会名额，理事单位 1 位免费参会名额。（本次会议属轮学盟工作会议，具体会议安排届时请参见会议通知）

二、人才培养活动计划

1.外智大师班

时间：5 月 15 日-16 日

地点：广州

会议费：6000 元，理事长单位、副理事长单位、智资委专家 7.5 折，理事单位 8.5 折

2.外智大师班

时间：11 月 17 日-20 日

地点：柳州

注册费：12000 元，理事长单位、副理事长单位、智资委专家 7.5 折，理事单位 8.5 折

协同创新、集聚资源、战略合作、
共策共力、突破瓶颈、互赢共荣

轮胎动力学通讯　2019 年第 4 期　总第 6 期
本期主编：卢荡
副主编：姚雪 陈晨 朱彦婷
2019 年 12 月 31 日